

Efficient evaluation of the material response of tissues reinforced by statistically oriented fibres

Original

Efficient evaluation of the material response of tissues reinforced by statistically oriented fibres / Hashlamoun, Kotaybah; Grillo, Alfio; Federico, Salvatore. - In: ZEITSCHRIFT FUR ANGEWANDTE MATHEMATIK UND PHYSIK. - ISSN 0044-2275. - 67:5(2016), p. 113. [10.1007/s00033-016-0704-5]

Availability:

This version is available at: 11583/2650667 since: 2020-06-03T00:11:40Z

Publisher:

Birkhauser Verlag AG

Published

DOI:10.1007/s00033-016-0704-5

Terms of use:

openAccess

This article is made available under terms and conditions as specified in the corresponding bibliographic description in the repository

Publisher copyright

Springer postprint/Author's Accepted Manuscript

This version of the article has been accepted for publication, after peer review (when applicable) and is subject to Springer Nature's AM terms of use, but is not the Version of Record and does not reflect post-acceptance improvements, or any corrections. The Version of Record is available online at: <http://dx.doi.org/10.1007/s00033-016-0704-5>

(Article begins on next page)

Efficient Evaluation of the Material Response of Tissues Reinforced by Statistically Oriented Fibres

Kotaybah Hashlamoun^a, Alfio Grillo^b, Salvatore Federico^{c,*}

^a Graduate Programme in Mechanical Engineering, The University of Calgary
2500 University Drive NW, Calgary, Alberta, T2N 1N4, Canada

^b DISMA - Department of Mathematical Sciences “G.L. Lagrange”, Politecnico di Torino
Corso Duca degli Abruzzi 24, 10124, Torino, Italy

^c Department of Mechanical and Manufacturing Engineering, The University of Calgary
2500 University Drive NW, Calgary, Alberta, T2N 1N4, Canada

* corresponding author:

Tel: +1-403-220-5790, Fax: +1-403-282-8406, Email: salvatore.federico@ucalgary.ca

Zeitschrift für Angewandte Mathematik und Physik 67, 113 (2016)

DOI: 10.1007/s00033-016-0704-5

Submitted 2016-01-14, accepted with revisions 2016-03-25, resubmitted 2016-07-27, accepted 2016-08-02, published 2016-08-25

1 Abstract

2 For several classes of soft biological tissues, modelling complexity is in part due to the arrangement
3 of the collagen fibres. In general, the arrangement of the fibres can be described by defining, at
4 each point in the tissue, the structure tensor (i.e., the tensor product of the unit vector of the local
5 fibre arrangement by itself) and a probability distribution of orientation. In this approach, assuming
6 that the fibres do not interact with each other, the overall contribution of the collagen fibres to
7 a given mechanical property of the tissue can be estimated by means of an averaging integral of
8 the constitutive function describing the mechanical property at study over the set of all possible
9 directions in space. Except for the particular case of fibre constitutive functions that are polynomial
10 in the transversely isotropic invariants of the deformation, the averaging integral cannot be evaluated
11 directly, in a single calculation because, in general, the integrand depends both on deformation and
12 on fibre orientation in a non-separable way. The problem is thus, in a sense, analogous to that of
13 solving the integral of a function of two variables, which cannot be split up into the product of two
14 functions, each depending only on one of the variables. Although numerical schemes can be used
15 to evaluate the integral at each deformation increment, this is computationally expensive. With the
16 purpose of containing computational costs, this work proposes approximation methods that are based
17 on the direct integrability of polynomial functions and that do not require the step-by-step evaluation
18 of the averaging integrals. Three different methods are proposed: *a*) a Taylor expansion of the fibre
19 constitutive function in the transversely isotropic invariants of the deformation; *b*) a Taylor expansion
20 of the fibre constitutive function in the structure tensor; *c*) for the case of a fibre constitutive function
21 having a polynomial argument, an approximation in which the directional average of the constitutive
22 function is replaced by the constitutive function evaluated at the directional average of the argument.
23 Each of the proposed methods approximates the averaged constitutive function in such a way that it is
24 multiplicatively decomposed into the product of a function of the deformation only and a function of
25 the structure tensors only. In order to assess the accuracy of these methods, we evaluate the constitutive
26 functions of the elastic potential and the Cauchy stress, for a biaxial test, under different conditions,
27 i.e., different fibre distributions and different ratios of the nominal strains in the two directions. The
28 results are then compared against those obtained for an averaging method available in the literature,
29 as well as against the integration made at each increment of deformation.

30 **Keywords:** biological tissue, collagen, fibre-reinforced, structure tensor, fabric tensor, averaging, Finite
31 Element Method, Continuum Mechanics, Elasticity

32 1. Introduction

33 Soft biological tissues can be seen as highly complex fibre-reinforced materials [1]. The solid phase
 34 can be represented by a mixture of an isotropic matrix and transversely isotropic fibres. The spatial
 35 arrangement of the fibres largely defines the anisotropy and inhomogeneity of the tissue (e.g., [2, 3]).
 36 In some tissues, the fibres can be thought of as being arranged in a finite number of families, each
 37 family being determined by the common direction of the fibres belonging to it. For instance, tissues
 38 typically modelled with a single fibre family are ligaments and tendons [4], and tissues with two fibre
 39 families are blood vessels [5, 6] and the atrium of the heart [7, 8].

40 However, the fibres usually have some dispersion with respect to the dominant direction(s) (e.g.,
 41 [6]). Moreover, there are tissues in which the dominant direction changes with location within the tissue
 42 or in which a dominant direction cannot be clearly defined. A prime example is articular cartilage,
 43 in which the fibre orientation varies along the depth of the tissue, from parallel to the surface in
 44 the superficial zone, to random in the middle zone (no dominant direction), to aligned to the depth
 45 direction in the deep zone [9, 10]. Whenever one wishes to consider the dispersion about the dominant
 46 direction(s) or tissues with more complex fibre orientations, it is necessary to describe the arrangement
 47 of the fibres by means of an infinite number of statistically oriented fibres, which requires the use of
 48 an orientation probability distribution.

49 Orientation probability distributions in Soft Tissue Biomechanics were first used by Lanir [11],
 50 and later adopted by several researchers (e.g., [12, 13, 14, 6]). Similar techniques were independently
 51 developed in the context of composite materials with inclusions [15, 16], and were subsequently trans-
 52 ferred to biomechanical problems such as the determination of the overall elastic properties or the
 53 overall permeability of soft tissues. These models were extended to the case of large deformations, at
 54 first for the elasticity alone [17] and then for both elasticity and permeability [18]. Here, we shall use
 55 the notation and concepts developed in these previous works.

56 For an extensive physical quantity, such as mass, momentum, energy, etc, the overall extent q of
 57 the quantity associated with the mixture as a whole is obtained as the weighted sum

$$q = \sum_{\alpha} \phi_{\alpha} q_{\alpha}, \quad (1)$$

58 where q_{α} is the value of the quantity in the constituent α and ϕ_{α} is the volumetric fraction of the
 59 constituent α . For lack of better knowledge, this *rule-of-mixture* can be extended also to quantities,
 60 such as the permeability, whose overall value may or may not be a linear combination as in Equation
 61 (1). We are interested in mixtures including one or more fibre families, each having statistical orienta-
 62 tion. The fibres in each family share the same properties but have different orientation, described by a
 63 probability distribution. Therefore, we think of each fibre family as an infinity of fibres, and evaluate
 64 its overall contribution by means of an integral over all directions in space. The overall contribution
 65 of each fibre family to a certain physical quantity, given by the averaging integral of the quantity, is
 66 called *fibre ensemble*.

67 The method proposed in [6], which we call GOH method (Gasser-Ogden-Holzapfel method),
 68 accounts for the overall effect of each family of statistically oriented fibres by means of the directional
 69 average of the material structure tensor (the tensor product of the unit vector representing the material
 70 fibre direction by itself). In their approach to the overall elastic properties of the arterial wall, after
 71 having defined a fibre elastic potential as a function of the structure tensor of a given direction, Gasser
 72 et al. [6] replaced the structure tensor by its directional average. The rule-of-mixture method gives the
 73 same results of the GOH method whenever the material property to be averaged is an affine function
 74 (i.e., a constant plus a linear function) in the structure tensor [17]. The GOH method has the advantage
 75 of requiring one single integration, directly. Indeed, once the probability distribution is known, the
 76 directional average of the structure tensor is a given tensor that has to be evaluated only once, and
 77 then used in all subsequent calculations. This makes the Finite Element (FE) implementation of the
 78 GOH method quite straightforward and, indeed, the GOH method is available in the material libraries
 79 of the commercially available software ABAQUS (Dassault Systèmes, Vélizy-Villacoublay, France).

80 In general, in the FE implementation of our rule-of-mixture method, the fibre ensemble (averaging
 81 integral of a certain physical quantity) must be calculated at each increment of deformation [17, 19].
 82 This is because of the coupled dependence of the integrand from *both* the structure tensor *and* the
 83 deformation.

84 Although sometimes fairly expensive from the computational point of view, an efficient numerical
 85 implementation of this method has been proposed [20], based on the use of spherical t -designs [21],
 86 in which the surface of the unit sphere is discretised into a suitable set of points, and the integral is
 87 evaluated as a summation on the discretised set of points. We recall that, since the oriented segment
 88 joining the centre of the unit sphere with a given point on its surface defines univocally a direction
 89 in space, the integration over the spherical surface can be made equivalent to integrating over all
 90 directions in space. Other numerical methods for finding the integration points on the surface of the
 91 sphere could be used (e.g., [22, 23, 24]), and a description of some of these methods can be found in
 92 [25]. However, a single, direct integration is possible whenever the integrand is a *separable function*
 93 of the deformation and the structure tensor, as is the case for *tensor-power polynomial* functions of
 94 the structure tensor (the definition of *tensor-power polynomial* is given later, in Section 2.3). We note
 95 that the GOH method is obtained in the instance of a tensor-power polynomial of degree one, which
 96 is an affine function of the structure tensor.

97 In this work, based on the direct integrability of polynomial functions, we introduce and com-
 98 pare three possible direct methods of approximation of the averaging integrals, with the purpose of
 99 estimating their accuracy, and establishing the ranges within which they perform as alternative op-
 100 tions to step-by-step integration criteria, while being computationally cheaper. We refer to these three
 101 methods as:

- 102 1. INEX (*Invariant Expansion*): the function to be averaged is viewed as a function of the invariants
 103 of the deformation that include the structure tensor, and then expanded in Taylor series about
 104 the values of the invariants in the reference configuration; then, the resulting polynomial is
 105 integrated;
- 106 2. STEX (*Structure Tensor Expansion*): the function to be averaged is expanded in Taylor series
 107 about the structure tensor of a convenient direction, and the resulting (tensor-power) polynomial
 108 is integrated;
- 109 3. PARG (*Polynomial Argument*): the function to be averaged is given by some function of an
 110 argument that is a (tensor-power) polynomial in the structure tensor, and the average is taken
 111 of the polynomial rather than of the whole function; in other words, the average is taken of
 112 the “outermost” argument that can be written as a (tensor-power) polynomial in the structure
 113 tensor.

114 These three methods are also compared with methods available in the literature:

- 115 4. GOH (*Gasser-Odgen-Holzappel*): the model proposed by Gasser et al. [6]; the GOH method can
 116 be seen as the extreme of our PARG method, in which the “innermost” argument is averaged:
 117 the structure tensor;
- 118 5. FESD (*Fibre Ensemble with Spherical Designs*): the step-by-step integration of the fibre ensemble
 119 of a certain physical quantity performed with the method of the spherical t -designs [20, 26].

120 The comparison is made based on a benchmark test in the context of elasticity, namely a biaxial
 121 tension test of a fibre-reinforced tissue sample, and the limitations of each methods are discussed.

122 2. Theoretical Background

123 We refer the Reader to the Appendix, where we briefly review the fairly standard Continuum Me-
 124 chanics notation that we use (Appendix A), recall the definitions of the invariants of the deformation
 125 for the cases of isotropy and transverse isotropy (Appendix B), as well as some basic relations in non-
 126 linear hyperelasticity (Appendix C), which will serve as our example of application of the averaging
 127 methods proposed in Section 3.

128 The notation follows that in a previous work [19], with a few small exceptions that allow for a
 129 lighter notation. The reference configuration of a body is denoted \mathcal{B} (rather than \mathcal{B}_R), the referential
 130 volumetric fraction of constituent α of a mixture is denoted Φ_α (rather than $\phi_{\alpha R}$), and the referential
 131 probability distribution of orientation of the fibres is denoted Ψ (rather than ψ).

132 In this section, we first recall the volumetric-distortional decomposition of the deformation, which
 133 we use for a purpose different than the usual one (quasi-incompressible materials), and introduce
 134 some definitions that are useful for the objectives of this work. Then, we introduce some important
 135 definitions in tensor algebra, and elucidate the averaging method based on the rule of mixtures that
 136 we employ in this work, and that gives rise to what we call the fibre ensemble. Finally, we recall the
 137 method by Gasser et al. [6] (GOH Method), to which we compare our results.

138 2.1. The Volumetric-Distortional Decomposition of the Deformation

139 The volumetric-distortional decomposition of the deformation gradient \mathbf{F} [27, 28, 29] is often employed
 140 in the treatment of quasi-incompressible materials. However, we shall use it for a different purpose,
 141 as outlined in Section 3.1. The deformation gradient tensor \mathbf{F} can be decomposed into its volumetric
 142 and distortional (or isochoric) part, $\mathbf{F} = J^{1/3}\bar{\mathbf{F}}$. We refer to $\bar{\mathbf{F}}$ as to the distortional (or isochoric)
 143 part of \mathbf{F} , since, by construction, it is characterised by having a unitary determinant, i.e., $\det \bar{\mathbf{F}} = 1$.
 144 Consistently, we decompose the right Cauchy-Green deformation tensor as $\mathbf{C} = J^{2/3}\bar{\mathbf{C}}$, where the
 145 isochoric part of \mathbf{C} is given by $\bar{\mathbf{C}} = \bar{\mathbf{F}}^T \cdot \bar{\mathbf{F}}$ and satisfies the equality $\det \bar{\mathbf{C}} = 1$.

146 2.2. Some Important Definitions in Tensor Algebra

147 Here, we introduce some definitions for the case of material tensors but, naturally, these are analogous
 148 for the case of spatial tensors. We indicate the full contraction of a material “contravariant” tensor
 149 \mathbb{T} and a material “covariant” tensor \mathbb{Z} of the same order r by means of the bra-ket notation $\langle \mathbb{T} | \mathbb{Z} \rangle =$
 150 $\mathbb{T}^{A_1 \dots A_r} \mathbb{Z}_{A_1 \dots A_r}$. Note that the bra-ket notation can be used symmetrically, i.e., $\langle \mathbb{T} | \mathbb{Z} \rangle = \langle \mathbb{Z} | \mathbb{T} \rangle$. For
 151 the particular case of second-order tensors, we can alternatively write $\mathbf{T} : \mathbf{Z} \equiv \langle \mathbf{T} | \mathbf{Z} \rangle = T^{AB} Z_{AB}$ and
 152 we call $\mathbf{T} : \mathbf{Z}$ the double contraction of \mathbf{T} and \mathbf{Z} .

153 Given any n material tensors $\mathbb{A}_1, \dots, \mathbb{A}_n$ of the same “contravariant” order r , “covariant” order s ,
 154 and overall order $r + s$, the *major-symmetric part* of the $n(r + s)$ -th order tensor

$$\mathbb{T} = \mathbb{A}_1 \otimes \dots \otimes \mathbb{A}_n \quad (2)$$

155 is given by

$$\text{msym}(\mathbb{T}) = \frac{1}{n!} \sum_{\sigma \in \mathfrak{S}_n} \mathbb{A}_{\sigma_1} \otimes \dots \otimes \mathbb{A}_{\sigma_n}, \quad (3)$$

156 where each $\sigma = \{\sigma_1, \dots, \sigma_n\}$ is one of all the $n!$ possible permutations \mathfrak{S}_n of $\{1, \dots, n\}$. Note that,
 157 if the tensors \mathbb{A}_i are of the first order (i.e., they are all vectors \mathbf{W}_i or all covectors $\mathbf{\Pi}_i$), then the
 158 major-symmetric part of \mathbb{T} coincides with its symmetric part.

159 For any material tensor \mathbb{A} (of any “contravariant” order r , “covariant” order s , and overall order
 160 $r + s$), its n -th tensor power is defined as the $n(r + s)$ -th order tensor

$$\mathbb{A}^{\otimes n} = \underbrace{\mathbb{A} \otimes \dots \otimes \mathbb{A}}_{n \text{ times}}, \quad (4)$$

161 and, by convention, we set $\mathbb{A}^{\otimes 1} = \mathbb{A}$ and $\mathbb{A}^{\otimes 0} = 1 \in \mathbb{R}$. Given two tensors \mathbb{A}, \mathbb{B} (of the same “con-
 162 travariant” order r , “covariant” order s , and overall order $r + s$), the binomial tensor power $(\mathbb{A} + \mathbb{B})^{\otimes n}$
 163 is given by the generalised Newton’s formula

$$(\mathbb{A} + \mathbb{B})^{\otimes n} = \sum_{k=0}^n \left[\binom{n}{k} \text{msym}(\mathbb{A}^{\otimes(n-k)} \otimes \mathbb{B}^{\otimes k}) \right], \quad (5)$$

164 where we recall that $\binom{n}{k}$ is the binomial coefficient $\binom{n}{k} = n! / (k!(n - k)!)$.

165 2.3. Materials with Statistically Oriented Fibres

166 Let \mathcal{F} be a generic physical quantity associated with a fibre-reinforced material, comprised of an
 167 isotropic matrix and anisotropic statistically oriented fibres. The considered quantity may be either a
 168 thermo-mechanical variable, such as stress, or a material property, such as stiffness or permeability.
 169 The mixture of matrix and fibres is assumed to be constrained, i.e., the matrix and fibres attain the
 170 same motion, with the same velocity \mathbf{v} and the same deformation gradient \mathbf{F} . For the sake of simplicity,
 171 we limit ourselves to the case of a single family of statistically oriented fibres. The orientation of the
 172 fibres is described by the probability $\Psi(\mathbf{M})$ to find a fibre in a given referential direction \mathbf{M} in the
 173 material unit sphere $\mathbb{S}^2\mathcal{B} = \{\mathbf{M} : \|\mathbf{M}\| = 1\}$. The probability density function Ψ is assumed to be
 174 invariant under the transformation $\mathbf{M} \mapsto -\mathbf{M}$, and normalised to one over the sphere, i.e. [30, 31],

$$\Psi(-\mathbf{M}) = \Psi(\mathbf{M}), \quad \int_{\mathbb{S}^2\mathcal{B}} \Psi(\mathbf{M}) = 1. \quad (6)$$

175 Note that we shall omit writing the ‘‘area element’’ or, more properly, the *area two-form* [32, 33] ‘‘dS’’
 176 in all surface integrals. If Φ_0 and Φ_1 are the referential volumetric fractions of the matrix and the
 177 fibres, respectively, the physical quantity \mathcal{F} can be written, in the reference configuration, with the
 178 rule-of-mixture expression

$$\mathcal{F} = \hat{\mathcal{F}}(\mathbf{C}, \Psi) = \Phi_0 \hat{\mathcal{F}}_0(\mathbf{C}) + \Phi_1 \int_{\mathbb{S}^2\mathcal{B}} \Psi(\mathbf{M}) \hat{\mathcal{F}}_1(\mathbf{C}, \mathbf{A}), \quad (7)$$

179 where $\mathbf{A} = \mathbf{M} \otimes \mathbf{M}$ is the structure tensor, $\hat{\mathcal{F}}$ is the constitutive function of \mathcal{F} , $\hat{\mathcal{F}}_0$ is the isotropic
 180 constitutive function of quantity \mathcal{F}_0 in the matrix, and $\hat{\mathcal{F}}_1$ is the anisotropic constitutive function of
 181 quantity \mathcal{F}_1 in the fibres. The integral

$$\mathcal{F}_e = \hat{\mathcal{F}}_e(\mathbf{C}, \Psi) = \int_{\mathbb{S}^2\mathcal{B}} \Psi(\mathbf{M}) \hat{\mathcal{F}}_1(\mathbf{C}, \mathbf{A}), \quad (8)$$

182 called the *fibre ensemble of \mathcal{F}_1* [18, 19], accounts for the effect of the fibres, and had initially been
 183 introduced for the case of the elastic potential [17].

184 In general, it is not possible to factorise the deformation \mathbf{C} out of the integral, and therefore the
 185 fibre ensemble cannot be calculated directly, but must be evaluated at each increment of deformation.
 186 This has been done [20] by means of the method of the spherical t -designs [21, 34], i.e., a set of N
 187 points $\{\mathbf{M}^{(1)}, \dots, \mathbf{M}^{(N)}\}$ in the material unit sphere $\mathbb{S}^2\mathcal{B}$ such that, for polynomials \mathcal{P} of degree $k \leq t$,

$$\int_{\mathbb{S}^2\mathcal{B}} \mathcal{P}(\mathbf{M}) = \frac{4\pi}{N} \sum_{r=1}^N \mathcal{P}(\mathbf{M}^{(r)}), \quad (9)$$

188 where 4π is the (surface) measure of the unit sphere $\mathbb{S}^2\mathcal{B}$. As mentioned in the Introduction, we shall
 189 denote the numerical integration of the rule-of-mixture expression of the fibre ensemble of Equation
 190 (8), performed with the method of the spherical designs, by the acronym FESD.

191 It is crucial to remark that a single, direct integration is possible when the constitutive function
 192 $\hat{\mathcal{F}}_1$ is a *separable* function of the structure tensor \mathbf{A} and the deformation \mathbf{C} . For a (scalar) constitutive
 193 function $\hat{\mathcal{F}}_1$, the most common case of separable function is a *tensor-power polynomial* in the structure
 194 tensor \mathbf{A} [19], of the type

$$\hat{\mathcal{F}}_1(\mathbf{C}, \mathbf{A}) = a \left[q_0(\mathbf{C}) + \sum_{p=1}^n \langle \mathbb{Q}_p(\mathbf{C}) | \mathbf{A}^{\otimes p} \rangle \right], \quad (10)$$

195 where a is a material constant with units of \mathcal{F}_1 , $q_0(\mathbf{C})$ is a non-dimensional scalar function of the
 196 deformation and the non-dimensional ‘‘covariant’’ tensor functions \mathbb{Q}_p are such that $\mathbb{Q}_p(\mathbf{C})$ is a tensor
 197 of order $2p$, which contracts with the ‘‘contravariant’’ tensor-power $\mathbf{A}^{\otimes p}$, which is the tensor of order
 198 $2p$ defined by

$$\mathbf{A}^{\otimes p} = \underbrace{\mathbf{A} \otimes \dots \otimes \mathbf{A}}_{p \text{ times}}. \quad (11)$$

199 Note that the tensors $\mathbb{Q}_p(\mathbf{C})$ and $\mathbf{A}^{\otimes p}$ are fully “covariant” and fully “contravariant”, respectively, which
 200 justifies the bra-ket notation, $\langle \cdot | \cdot \rangle$. For the constitutive function in Equation (10), it is possible to
 201 exploit the linearity of the integration operator and to factorise the deformation out of each resulting
 202 integral, so that the fibre ensemble of Equation (8) becomes [19]

$$\mathcal{F}_e = \hat{\mathcal{F}}_e(\mathbf{C}, \Psi) = a \left[q_0(\mathbf{C}) + \sum_{p=1}^n \langle \mathbb{Q}_p(\mathbf{C}) | \mathbb{H}_p \rangle \right], \quad (12)$$

203 where we define the averaged structure tensor of order $2p$ as [30, 31, 19, 35]

$$\mathbb{H}_p = \int_{\mathbb{S}^{2B}} \Psi(\mathbf{M}) \mathbf{A}^{\otimes p}. \quad (13)$$

204 Therefore, an analytical form of the fibre ensemble can be obtained as a function of the deformation
 205 \mathbf{C} and can be introduced directly into a Finite Element implementation, without the need to calculate
 206 an integral at each increment of deformation.

207 We shall exploit the property of direct integrability of polynomial constitutive functions to pro-
 208 pose our integration methods in Section 3.

209 **Remark.** We refer to the constitutive function of Equation (10) as to a tensor-power polynomial
 210 because the *tensor power* $\mathbf{A}^{\otimes p}$ is involved, rather than the regular power \mathbf{A}^p . Indeed, because of the
 211 *idempotence* of \mathbf{A} [36, 37], the regular power would lead to the trivial result $\mathbf{A}^p = \mathbf{A}$, which means
 212 that any (regular) polynomial of the N -th order in \mathbf{A} would reduce to an affine function in \mathbf{A} . The
 213 idempotence of \mathbf{A} can be shown in components:

$$(\mathbf{A}^2)^{AD} = A^{AB} G_{BC} A^{CD} = M^A M^B G_{BC} M^C M^D = M^A M^D = A^{AD}. \quad (14)$$

214 Furthermore, we note that, for a second-order tensor, whereas the regular power is an *internal* oper-
 215 ation, the tensor power is an *external* operation, in so far as its result is a tensor of different order
 216 than the original one. A particularly interesting case occurs when the $2p$ -th order tensor $\mathbb{Q}_p(\mathbf{C})$ can be
 217 written as the tensor product of p tensors of order two. An even more peculiar situation occurs when
 218 it holds that $\mathbb{Q}_p(\mathbf{C}) = q_p(\mathbf{C}) \mathbf{C}^{\otimes p}$, for every $p \in \{1, \dots, N\}$, with $q_p(\mathbf{C})$ being a suitable scalar-valued
 219 function of \mathbf{C} , so that Equation (10) becomes

$$\hat{\mathcal{F}}_1(\mathbf{C}, \mathbf{A}) = a \left[q_0(\mathbf{C}) + \sum_{p=1}^n q_p(\mathbf{C}) \langle \mathbf{C}^{\otimes p} | \mathbf{A}^{\otimes p} \rangle \right]. \quad (15)$$

220 Because of the identity

$$I_4^p = (\mathbf{C} : \mathbf{A})^p = \langle \mathbf{C} | \mathbf{A} \rangle^p = \langle \mathbf{C}^{\otimes p} | \mathbf{A}^{\otimes p} \rangle, \quad (16)$$

221 the expression (15) becomes a polynomial of degree N in the fourth invariant $I_4 = \langle \mathbf{C} | \mathbf{A} \rangle = \mathbf{C} : \mathbf{A}$,
 222 i.e.,

$$\hat{\mathcal{F}}_1(\mathbf{C}, \mathbf{A}) = \check{\mathcal{F}}_1(I_4) = q_0(\mathbf{C}) + \sum_{p=1}^N q_p(\mathbf{C}) I_4^p. \quad (17)$$

223 2.4. Averaged Structure Tensors \mathbb{H}_p of Order $2p$

224 To the best of our knowledge, the generalised structure tensors that we denote \mathbb{H}_p in Equation (13)
 225 were first introduced by Kanatani [30], who actually called “fabric tensors” the *deviatoric* parts of the
 226 \mathbb{H}_p , with some normalisation constants (cf., in [30], Equation (3.4), which corresponds exactly to the
 227 definition of \mathbb{H}_p , and Equation (3.3), which defines Kanatani’s “fabric tensors”). Advani and Tucker
 228 [31] noted that all averaged structure tensors of order smaller than $p \geq 2$ can be found from \mathbb{H}_p by
 229 contracting pairs of its indices (which, in our formalism, requires the use of the metric tensor), as it
 230 can be shown, e.g., in components. Our group first employed the tensors \mathbb{H}_p only recently [19] and,
 231 regretfully, we were unaware of the works by Kanatani [30] and Advani and Tucker [31] at that time.

232 For $p = 1$, the averaged tensor in Equation (13) coincides with the second-order tensor given by the
 233 average of the structure tensor \mathbf{A} ,

$$\mathbf{H} = \int_{\mathbb{S}^2\mathcal{B}} \Psi(\mathbf{M}) \mathbf{A}, \quad (18)$$

234 which Gasser et al. [6] called ‘‘generalised structure tensor’’ and used as the basis of their averaging
 235 method (see Section 2.5). In the following, we will generally use the identification $\mathbb{H}_1 \equiv \mathbf{H}$, except in
 236 sums over p involving the tensors \mathbb{H}_p of order $2p$. To our knowledge, prior to this work, the fourth-order
 237 averaged structure tensor \mathbb{H}_2 was used in biomechanics by Vasta et al. [38] and Gizzi et al. [39], who
 238 called it simply \mathbb{H} .

239 2.5. The Gasser-Ogden-Holzapfel Method (GOH)

240 The method proposed by Gasser et al. [6], thereby called GOH method, allows for a single, direct
 241 integration, and we describe it here in our notation. Gasser et al. [6] proposed to evaluate the overall
 242 effect of the fibres on a physical quantity \mathcal{F} by replacing the structure tensor \mathbf{A} in the fibre function
 243 $\mathcal{F}_1 = \hat{\mathcal{F}}_1(\mathbf{C}, \mathbf{A})$ by means of its directional average \mathbf{H} introduced in Equation (18), to obtain

$$\mathcal{F}_{\text{GOH}} = \hat{\mathcal{F}}_{\text{GOH}}(\mathbf{C}, \Psi) = \hat{\mathcal{F}}_1(\mathbf{C}, \mathbf{H}), \quad (19)$$

244 which they used in Equation (7) in place of our fibre ensemble $\hat{\mathcal{F}}_e$ of Equation (8). When $\hat{\mathcal{F}}_1$ is affine
 245 in the structure tensor \mathbf{A} , i.e., it is a (tensor-power) polynomial of degree one in \mathbf{A} ,

$$\hat{\mathcal{F}}_1(\mathbf{C}, \mathbf{A}) = a [q_0(\mathbf{C}) + \mathbf{Q}(\mathbf{C}) : \mathbf{A}], \quad (20)$$

246 where a is a constant, q_0 is a scalar function of \mathbf{C} , and \mathbf{Q} is a second-order ‘‘covariant’’ tensor-valued
 247 function of \mathbf{C} , we have

$$\begin{aligned} \hat{\mathcal{F}}_e(\mathbf{C}, \Psi) &= \int_{\mathbb{S}^2\mathcal{B}} \Psi(\mathbf{M}) \hat{\mathcal{F}}_1(\mathbf{C}, \mathbf{A}) = \int_{\mathbb{S}^2\mathcal{B}} \Psi(\mathbf{M}) a [q_0(\mathbf{C}) + \mathbf{Q}(\mathbf{C}) : \mathbf{A}] \\ &= a \left[q_0(\mathbf{C}) + \mathbf{Q}(\mathbf{C}) : \left(\int_{\mathbb{S}^2\mathcal{B}} \Psi(\mathbf{M}) \mathbf{A} \right) \right] = a [q_0(\mathbf{C}) + \mathbf{Q}(\mathbf{C}) : \mathbf{H}] \\ &= \hat{\mathcal{F}}_1(\mathbf{C}, \mathbf{H}) = \hat{\mathcal{F}}_{\text{GOH}}(\mathbf{C}, \Psi), \end{aligned} \quad (21)$$

248 i.e., the rule-of-mixture method coincides with the GOH method [17].

249 3. Approximation of the Fibre Ensemble

250 Here we introduce three methods that provide analytical approximations of the fibre ensemble (8),
 251 all based on the fact that, for a fibre function $\hat{\mathcal{F}}_1$ that is a tensor-power polynomial in the structure
 252 tensor, a single, direct integration is possible [19]. Two of the proposed methods are based on the
 253 Taylor expansion of the fibre function $\hat{\mathcal{F}}_1$, in order to obtain polynomial functions in the structure
 254 tensor \mathbf{A} . In the first method, we expand in the transversely isotropic invariants, which are linear
 255 functions of \mathbf{A} (see Equation (72)). In the second method, we expand in the structure tensor \mathbf{A} . In
 256 the third method, in a fashion similar to that of the GOH method [6], for the case of a fibre function
 257 $\hat{\mathcal{F}}_1$ that is a function of a tensor-power polynomial $\mathcal{P}(\mathbf{A})$, we replace the fibre ensemble by the same
 258 function evaluated at the directional average of $\mathcal{P}(\mathbf{A})$, which can be calculated directly.

259 3.1. Taylor Expansion in the Invariants (INEX)

260 Let $\check{\mathcal{F}}_1(I_1, I_2, I_3, I_4, I_5) = \hat{\mathcal{F}}_1(\mathbf{C}, \mathbf{A})$ be the fibre constitutive function written as a function of the five
 261 transversely isotropic invariants (when looking at a single direction \mathbf{M} , the symmetry is naturally
 262 that of transverse isotropy). For the sake of a lighter notation, let us omit writing the three isotropic
 263 invariants I_1, I_2, I_3 among the arguments of $\check{\mathcal{F}}_1$ and, for the sake of a simpler presentation, let us
 264 assume that $\check{\mathcal{F}}_1$ does not depend on the fifth invariant I_5 . If I_5 were included, the derivation would
 265 be analogous, but lengthier, and the Taylor expansion formulae would require the introduction of the
 266 multi-index notation. Furthermore, we write $I_4 = J^{2/3} \bar{I}_4$, i.e., we express I_4 in terms of its purely

267 distortional counterpart \bar{I}_4 . Therefore, let us write the fibre quantity \mathcal{F}_1 as a constitutive function of
 268 J and \bar{I}_4 , i.e.,

$$\mathcal{F}_1 = \hat{\mathcal{F}}_1(\mathbf{C}, \mathbf{A}) = \check{\mathcal{F}}_1(J, \bar{I}_4). \quad (22)$$

269 We remark that, although we omitted indicating explicitly the dependence of $\check{\mathcal{F}}_1$ on $I_3 = J^2$, in the
 270 sequel we express $\check{\mathcal{F}}_1$ as a function of \bar{I}_4 and J in order to emphasise that J is used to express I_4 as
 271 $J^{2/3}\bar{I}_4$. We also remark that we are *not* decomposing I_4 into its volumetric and distortional parts in
 272 order to impose incompressibility, which is the most common case in which one uses the volumetric-
 273 distortional decomposition, but because it serves our purpose of a Taylor expansion at a point of zero
 274 (distortional) deformation, as it will be explained later.

275 For a given $\mathbf{C} = J^{2/3}\bar{\mathbf{C}}$, it is fairly straightforward to prove that the admissible values of I_4
 276 and \bar{I}_4 belong to the closed intervals $\Lambda(\mathbf{C}) = [\lambda_{\min}^2, \lambda_{\max}^2]$ and $\Lambda(\bar{\mathbf{C}}) = [\bar{\lambda}_{\min}^2, \bar{\lambda}_{\max}^2]$, respectively,
 277 where λ_{\min}^2 and λ_{\max}^2 are the minimum and maximum eigenvalue of \mathbf{C} , and $\bar{\lambda}_{\min}^2$ and $\bar{\lambda}_{\max}^2$ are those
 278 of $\bar{\mathbf{C}}$ (see Appendix D for both an analytical and graphical proof). Note that, in the undeformed
 279 configuration, for which $\mathbf{C} = \bar{\mathbf{C}} = \mathbf{G}$ (where the metric tensor \mathbf{G} serves as the ‘‘covariant’’ identity
 280 tensor), the intervals $\Lambda(\mathbf{C})$ and $\Lambda(\bar{\mathbf{C}})$ degenerate into the singleton $\Lambda(\mathbf{G}) = \{1\}$. We also remark
 281 that the admissible intervals of I_5 and \bar{I}_5 have the same form of those of I_4 and \bar{I}_4 , except that the
 282 exponents 2 of the maximum and minimum stretches have to be replaced by exponents 4.

283 For our purposes, it is very important to note that it is *always* verified that $\bar{I}_{40} = 1 \in \Lambda(\bar{\mathbf{C}}) =$
 284 $[\bar{\lambda}_{\min}^2, \bar{\lambda}_{\max}^2]$. Indeed, the condition $\det \bar{\mathbf{C}} = 1$ implies that $\bar{\lambda}_{\min}^2 < 1$ and $\bar{\lambda}_{\max}^2 > 1$. Therefore, if $\check{\mathcal{F}}_1$
 285 belongs to the space $C^n(\mathring{\Lambda}(\bar{\mathbf{C}}))$ of continuously differentiable functions up to order n in the open set
 286 $\mathring{\Lambda}(\bar{\mathbf{C}}) =]\bar{\lambda}_{\min}^2, \bar{\lambda}_{\max}^2[$ of the interior points of $\Lambda(\bar{\mathbf{C}})$, it is possible to approximate $\check{\mathcal{F}}_1$ by means of a
 287 Taylor expansion in the variable \bar{I}_4 , about the value $\bar{I}_{40} = 1 \in \Lambda(\bar{\mathbf{C}})$. For this purpose, we invoke the
 288 Taylor’s expansion formula of order n for $\check{\mathcal{F}}_1$, which reads

$$\check{\mathcal{F}}_1(J, \bar{I}_4) = \check{\mathcal{T}}_n(J, \bar{I}_4) + \check{\mathcal{R}}_n(J, \bar{I}_4) = \sum_{j=0}^n \frac{1}{j!} \frac{\partial^{(j)} \check{\mathcal{F}}_1}{\partial \bar{I}_4^{(j)}}(J, 1) [\bar{I}_4 - 1]^j + \check{\mathcal{R}}_n(J, \bar{I}_4), \quad (23)$$

289 where $\check{\mathcal{T}}_n(J, \bar{I}_4)$ is the Taylor polynomial of order n associated with $\check{\mathcal{F}}_1$ at $1 \in \mathring{\Lambda}(\bar{\mathbf{C}})$. If $\check{\mathcal{F}}_1$ is differen-
 290 tiable $n + 1$ times in $\mathring{\Lambda}(\bar{\mathbf{C}}) \setminus \{1\}$, the remainder $\check{\mathcal{R}}_n(\bar{I}_4)$ can be given in Lagrange’s form as

$$\check{\mathcal{R}}_n(J, \bar{I}_4) = \frac{1}{(n+1)!} \frac{\partial^{(n+1)} \check{\mathcal{F}}_1}{\partial \bar{I}_4^{(n+1)}}(J, \xi_{n+1}) [\bar{I}_4 - 1]^{n+1}, \quad (24)$$

291 for some $\xi_{n+1} \in \mathring{\Lambda}(\bar{\mathbf{C}})$ lying between 1 and \bar{I}_4 , and depending on \bar{I}_4 as well as on the order n of the
 292 expansion.

293 We now exploit $\bar{I}_4 = \bar{\mathbf{C}} : \mathbf{A} = J^{-2/3} \mathbf{C} : \mathbf{A}$, and write the Taylor polynomial and the remainder
 294 as explicit functions of the structure tensor \mathbf{A} , i.e.,

$$\check{\mathcal{T}}_n(J, \bar{I}_4) = \hat{\mathcal{T}}_n(\mathbf{C}, \mathbf{A}) = \sum_{j=0}^n \frac{1}{j!} \frac{\partial^{(j)} \check{\mathcal{F}}_1}{\partial \bar{I}_4^{(j)}}(J, 1) [J^{-2/3} \mathbf{C} : \mathbf{A} - 1]^j, \quad (25a)$$

$$\check{\mathcal{R}}_n(J, \bar{I}_4) = \hat{\mathcal{R}}_n(\mathbf{C}, \mathbf{A}) = \frac{1}{(n+1)!} \frac{\partial^{(n+1)} \check{\mathcal{F}}_1}{\partial \bar{I}_4^{(n+1)}}(J, \xi_{n+1}) [J^{-2/3} \mathbf{C} : \mathbf{A} - 1]^{n+1}, \quad (25b)$$

295 which give

$$\hat{\mathcal{F}}_1(\mathbf{C}, \mathbf{A}) = \hat{\mathcal{T}}_n(\mathbf{C}, \mathbf{A}) + \hat{\mathcal{R}}_n(\mathbf{C}, \mathbf{A}). \quad (26)$$

296 Then, we multiply both sides of Equation (26) by the probability distribution $\Psi(\mathbf{M})$, integrate over
 297 the material sphere $\mathbb{S}^2\mathcal{B}$, and obtain

$$\mathcal{F}_e = \mathcal{G}_n + \mathcal{E}_n, \quad (27)$$

298 where \mathcal{F}_e is the fibre ensemble of Equation (8), and

$$\mathcal{G}_n = \int_{\mathbb{S}^2\mathcal{B}} \Psi(\mathbf{M}) \hat{\mathcal{T}}_n(\mathbf{C}, \mathbf{A}), \quad (28a)$$

$$\mathcal{E}_n = \int_{\mathbb{S}^2\mathcal{B}} \Psi(\mathbf{M}) \hat{\mathcal{R}}_n(\mathbf{C}, \mathbf{A}), \quad (28b)$$

299 are the n -th order approximation of \mathcal{F}_e and the corresponding error \mathcal{E}_n , which is entirely defined by
300 the difference $\mathcal{E}_n := \mathcal{F}_e - \mathcal{G}_n$. Equation (28a) defines the sequence $\{\mathcal{G}_n\}_{n \in \mathbb{N}}$, in which \mathcal{G}_n is given by

$$\begin{aligned} \mathcal{G}_n = \hat{\mathcal{G}}_n(\mathbf{C}, \Psi) &= \sum_{j=0}^n \frac{1}{j!} \frac{\partial^{(j)} \check{\mathcal{F}}_1}{\partial \bar{\mathbf{I}}_4^{(j)}}(J, 1) \int_{\mathbb{S}^2\mathcal{B}} \Psi(\mathbf{M}) [J^{-2/3} \mathbf{C} : \mathbf{A} - 1]^j \\ &= \sum_{j=0}^n \frac{1}{j!} \frac{\partial^{(j)} \check{\mathcal{F}}_1}{\partial \bar{\mathbf{I}}_4^{(j)}}(J, 1) \sum_{k=0}^j \binom{j}{k} (-1)^k (J^{-2/3})^{j-k} \int_{\mathbb{S}^2\mathcal{B}} \Psi(\mathbf{M}) [\mathbf{C} : \mathbf{A}]^{j-k}. \end{aligned} \quad (29)$$

301 The Cauchy-Green deformation tensor \mathbf{C} can be factorised out of the integral sign in (29) by using
302 the identity (16), from which

$$\int_{\mathbb{S}^2\mathcal{B}} \Psi(\mathbf{M}) [\mathbf{C} : \mathbf{A}]^{j-k} = \langle \mathbf{C}^{\otimes(j-k)} | \mathbb{H}_{j-k} \rangle. \quad (30)$$

303 By virtue of this result, the n -th order approximation of \mathcal{F}_e can be recast in the compact form

$$\mathcal{G}_n = \hat{\mathcal{G}}_n(\mathbf{C}, \Psi) = \sum_{j=0}^n \frac{1}{j!} \frac{\partial^{(j)} \check{\mathcal{F}}_1}{\partial \bar{\mathbf{I}}_4^{(j)}}(J, 1) \sum_{k=0}^j \binom{j}{k} (-1)^k (J^{-2/3})^{j-k} \langle \mathbf{C}^{\otimes(j-k)} | \mathbb{H}_{j-k} \rangle, \quad (31)$$

304 in which the deformation has been completely factorised with respect to directional averaging, the
305 latter being accounted for by the averaged structure tensor of order $2(j-k)$, \mathbb{H}_{j-k} . To estimate
306 the error, let us consider for simplicity the case in which \mathcal{F}_1 is a scalar constitutive function, so
307 that its associated fibre ensemble, \mathcal{F}_e , and n -th order approximation, \mathcal{G}_n , are scalars too. If the error
308 $\mathcal{E}_n = \mathcal{F}_e - \mathcal{G}_n$ vanishes as n goes towards infinity, \mathcal{F}_e can be represented exactly by the limit $\lim_{n \rightarrow \infty} \mathcal{G}_n$,
309 in which case it holds that

$$\mathcal{F}_e = \lim_{n \rightarrow \infty} \mathcal{G}_n. \quad (32)$$

310 To estimate \mathcal{E}_n , we follow the theory of Taylor expansion formulae, and we infer that, if there exist
311 positive constants L and Q , such that

$$\left| \frac{\partial^{n+1} \check{\mathcal{F}}_1}{\partial \bar{\mathbf{I}}_4^{n+1}}(J, \bar{\mathbf{I}}_4) \right| \leq L Q^{n+1}, \quad \forall \bar{\mathbf{I}}_4 \in \mathring{\Delta}(\bar{\mathbf{C}}), \quad (33)$$

312 then it holds that

$$|\mathcal{E}_n| \leq \int_{\mathbb{S}^2\mathcal{B}} \Psi(\mathbf{M}) \left| \hat{\mathcal{R}}_n(\mathbf{C}, \mathbf{A}) \right| \leq L \frac{Q^{n+1}}{(n+1)!} \int_{\mathbb{S}^2\mathcal{B}} \Psi(\mathbf{M}) |\bar{\mathbf{I}}_4 - 1|^{n+1} \leq L \frac{Q^{n+1} (\bar{\lambda}_{\max}^2 - \bar{\lambda}_{\min}^2)^{n+1}}{(n+1)!}. \quad (34)$$

313 Note that, in the case in which \mathcal{F}_1 is a tensor-valued constitutive quantity, the estimates (33) and (34)
314 must be generalised by replacing the absolute value with an appropriate norm.

315 For a sufficiently high order n of the Taylor's expansion (23), we enforce the approximation

$$\mathcal{F}_e \simeq \mathcal{G}_n, \quad (35)$$

316 the accuracy of which increases when the absolute value of the error, $|\mathcal{E}_n|$, tends towards zero. For
317 example, this is the case when $\bar{\lambda}_{\max}^2$ and $\bar{\lambda}_{\min}^2$ tend to be equal to each other.

318 Equations (27) and (35) constitute the INEX (Invariant Expansion) method, and provide a
319 polynomial approximation of the fibre ensemble $\hat{\mathcal{F}}_e$, *regardless* of the form of the orientation probability
320 distribution Ψ . This is achieved by expanding the fibre constitutive function $\check{\mathcal{F}}_1(J, \cdot)$ about $\bar{\mathbf{I}}_4 = 1$,
321 which rules out any dependence on a ‘‘privileged’’ direction \mathbf{M}_0 . In order to clearly show this, let
322 \mathbf{M}_0 be any direction, with the associated structure tensor $\mathbf{A}_0 = \mathbf{M}_0 \otimes \mathbf{M}_0$. Since $\bar{\mathbf{I}}_4 = \bar{\mathbf{C}} : \mathbf{A}_0$,

323 when $\bar{\mathbf{C}} = \mathbf{G}$, we have that $\bar{I}_{40} = 1$, for every \mathbf{M}_0 . Therefore, the INEX approximation is valid for
 324 any orientation distribution Ψ . This is in contrast with the STEX method presented in Section 3.2,
 325 which is based on the expansion about $\mathbf{A}_0 = \mathbf{M}_0 \otimes \mathbf{M}_0$, and is thus accurate *only* for orientation
 326 distributions Ψ with small dispersions about \mathbf{M}_0 . We observed that the INEX method gave the best
 327 results for even orders of expansion.

328 3.2. Taylor Expansion in the Structure Tensor (STEX)

329 Given a fibre function $\mathcal{F}_1 = \hat{\mathcal{F}}_1(\mathbf{C}, \mathbf{A})$ and a structure tensor $\mathbf{A}_0 = \mathbf{M}_0 \otimes \mathbf{M}_0$, if $\hat{\mathcal{F}}_1$ is of class C^n in
 330 a neighbourhood of \mathbf{A}_0 , it is possible to use Taylor's expansion formula in \mathbf{A} about \mathbf{A}_0 ,

$$\hat{\mathcal{F}}_1(\mathbf{C}, \mathbf{A}) = \hat{\mathcal{T}}_n(\mathbf{C}, \mathbf{A}) + \hat{\mathcal{R}}_n(\mathbf{C}, \mathbf{A}) = \sum_{j=0}^n \frac{1}{j!} \left\langle \frac{\partial^{(j)} \hat{\mathcal{F}}_1}{\partial \mathbf{A}^{(j)}}(\mathbf{C}, \mathbf{A}_0) \middle| (\mathbf{A} - \mathbf{A}_0)^{\otimes j} \right\rangle + \hat{\mathcal{R}}_n(\mathbf{C}, \mathbf{A}), \quad (36)$$

331 where, similarly to the case of the INEX method, $\hat{\mathcal{T}}_n(\mathbf{C}, \mathbf{A})$ is the Taylor polynomial of order n , and
 332 if $\hat{\mathcal{F}}_1$ is of class C^{n+1} in \mathbf{A} , the remainder $\hat{\mathcal{R}}_n(\mathbf{C}, \mathbf{A})$ can be expressed in Lagrange's form (we omit
 333 the details).

334 Multiplying both sides of Equation (36) by the probability density Ψ and then integrating over
 335 the material sphere $\mathbb{S}^2\mathcal{B}$, we obtain

$$\mathcal{F}_e = \mathcal{G}_n + \mathcal{E}_n, \quad (37)$$

336 where, analogously to the case of the INEX method, \mathcal{F}_e is the fibre ensemble of Equation (8), \mathcal{G}_n is
 337 the n -th order approximation of \mathcal{F}_e and \mathcal{E}_n is the n -th order error, defined formally as in Equations
 338 (28a) and (28b). The term \mathcal{G}_n of the sequence $\{\mathcal{G}_n\}_{n \in \mathbb{N}}$ is given by

$$\begin{aligned} \mathcal{G}_n = \hat{\mathcal{G}}_n(\mathbf{C}, \Psi) &= \int_{\mathbb{S}^2\mathcal{B}} \left[\Psi(\mathbf{M}) \sum_{j=0}^n \frac{1}{j!} \left\langle \frac{\partial^{(j)} \hat{\mathcal{F}}_1}{\partial \mathbf{A}^{(j)}}(\mathbf{C}, \mathbf{A}_0) \middle| (\mathbf{A} - \mathbf{A}_0)^{\otimes j} \right\rangle \right] \\ &= \sum_{j=0}^n \frac{1}{j!} \left\langle \frac{\partial^{(j)} \hat{\mathcal{F}}_1}{\partial \mathbf{A}^{(j)}}(\mathbf{C}, \mathbf{A}_0) \middle| \int_{\mathbb{S}^2\mathcal{B}} \Psi(\mathbf{M}) (\mathbf{A} - \mathbf{A}_0)^{\otimes j} \right\rangle. \end{aligned} \quad (38)$$

339 Note that the integrals on the right-hand side of the bra-ket are independent of the deformation \mathbf{C} .
 340 Using the expression (5) of the binomial tensor power and the linearity of the integral operation, it is
 341 possible to write Equation (38) in the form

$$\mathcal{F}_e \simeq \mathcal{G}_n = \hat{\mathcal{G}}_n(\mathbf{C}, \Psi) = \sum_{j=0}^n \frac{1}{j!} \left\langle \frac{\partial^{(j)} \hat{\mathcal{F}}_1}{\partial \mathbf{A}^{(j)}}(\mathbf{C}, \mathbf{A}_0) \middle| \sum_{k=0}^j [(-1)^k \binom{j}{k} \text{msym}(\mathbb{H}_{j-k} \otimes \mathbf{A}_0^{\otimes k})] \right\rangle, \quad (39)$$

342 which features the averaged structure tensors \mathbb{H}_p of Equation (13). Equations (37) and (39) yield
 343 an analytical approximation of the fibre potential \mathcal{F}_e as a function of the deformation \mathbf{C} . It seems
 344 natural to expand about the structure tensor $\mathbf{A}_0 = \mathbf{M}_0 \otimes \mathbf{M}_0$ relative to the dominant direction \mathbf{M}_0
 345 of the fibres, in which case the best results are obtained when the dispersion of the fibres about that
 346 direction is relatively small. We note that Vasta et al. [38] have in fact implemented what here we
 347 would call the STEX method of order 2, i.e., involving only $\mathbb{H}_1 \equiv \mathbf{H}$ and \mathbb{H}_2 . Also in this case, the
 348 best results were obtained for even orders of expansion.

349 3.3. Polynomial Argument Method (PARG)

350 In this section, we consider a fibre function of the type

$$\mathcal{F}_1 = \hat{\mathcal{F}}_1(\mathbf{C}, \mathbf{A}) = \mathfrak{f}(\mathcal{P}(\mathbf{C}, \mathbf{A})), \quad (40)$$

351 where \mathfrak{f} describes the physical quantity that has to be modelled (e.g., the elastic potential) and $\mathcal{P}(\mathbf{C}, \mathbf{A})$
 352 is defined by the N -th degree *tensor-power polynomial*

$$\mathcal{P}(\mathbf{C}, \mathbf{A}) := q_0(\mathbf{C}) + \sum_{p=1}^N \langle \mathbb{Q}_p(\mathbf{C}) | \mathbf{A}^{\otimes p} \rangle, \quad (41)$$

353 in which, as in Equation (10), q_0 and \mathbb{Q}_p are, respectively, a non-dimensional scalar-valued func-
 354 tion and a non-dimensional ‘‘covariant’’ tensor-valued function of order $2p$ of the right Cauchy-Green
 355 deformation tensor. We propose to approximate the fibre ensemble as

$$\mathcal{F}_e = \hat{\mathcal{F}}_e(\mathbf{C}, \Psi) = \int_{\mathbb{S}^2\mathcal{B}} \Psi(\mathbf{M}) \mathfrak{f}(\mathcal{P}(\mathbf{C}, \mathbf{A})) \simeq \mathfrak{f} \left(\int_{\mathbb{S}^2\mathcal{B}} \Psi(\mathbf{M}) \mathcal{P}(\mathbf{C}, \mathbf{A}) \right). \quad (42)$$

356 This approximation becomes exact if the operation of directional averaging commutes with the function
 357 \mathfrak{f} . This holds true, for example, when \mathfrak{f} is a polynomial of degree M in $\mathcal{P}(\mathbf{C}, \mathbf{A})$, and $\mathcal{P}(\mathbf{C}, \mathbf{A})$ is
 358 expressed as the $\hat{\mathcal{F}}_1$ of Equation (15), with $\mathbb{Q}_p(\mathbf{C}) = q_p(\mathbf{C}) \mathbf{C}^{\otimes p}$, and $q_p(\mathbf{C})$ scalar functions of \mathbf{C} , so
 359 that $\mathcal{P}(\mathbf{C}, \mathbf{A})$ can be written as a polynomial in I_4 :

$$\mathcal{P}(\mathbf{C}, \mathbf{A}) = \check{\mathcal{P}}(I_4) = q_0(\mathbf{C}) + \sum_{p=1}^N q_p(\mathbf{C}) I_4^p. \quad (43)$$

360 With these assumptions, $\mathfrak{f}(\mathcal{P}(\mathbf{C}, \mathbf{A}))$ can be reformulated as a polynomial of degree MN in I_4 , i.e.,

$$\hat{\mathcal{F}}_1(\mathbf{C}, \mathbf{A}) = \mathfrak{f}(\mathcal{P}(\mathbf{C}, \mathbf{A})) = \mathfrak{f}(\check{\mathcal{P}}(I_4)) = a_0(\mathbf{C}) + \sum_{h=1}^{MN} a_h(\mathbf{C}) I_4^h = a_0(\mathbf{C}) + \sum_{h=1}^{MN} a_h(\mathbf{C}) \langle \mathbf{C} | \mathbf{A} \rangle^h, \quad (44)$$

361 where each function a_h , with $h \in \{0, \dots, MN\}$, is obtained by combining the functions q_p of (17)
 362 with the coefficients of the polynomial expressing \mathfrak{f} . By using the identity (16), which leads to

$$\int_{\mathbb{S}^2\mathcal{B}} \Psi(\mathbf{M}) \langle \mathbf{C} | \mathbf{A} \rangle^h = \left\langle \mathbf{C}^{\otimes h} \left| \int_{\mathbb{S}^2\mathcal{B}} \Psi(\mathbf{M}) \mathbf{A}^{\otimes h} \right. \right\rangle = \langle \mathbf{C}^{\otimes h} | \mathbb{H}_h \rangle, \quad (45)$$

363 the fibre ensemble can be expressed exactly in terms of the averaged generalised structure tensors \mathbb{H}_h ,
 364 i.e.,

$$\mathcal{F}_e = \int_{\mathbb{S}^2\mathcal{B}} \Psi(\mathbf{M}) \hat{\mathcal{F}}_1(\mathbf{C}, \mathbf{A}) = a_0(\mathbf{C}) + \sum_{h=1}^{MN} a_h(\mathbf{C}) \langle \mathbf{C}^{\otimes h} | \mathbb{H}_h \rangle. \quad (46)$$

365 In general, however, for arbitrary functions \mathfrak{f} , the approximation (42) is exact in the limit $\mathbf{C} \rightarrow \mathbf{G}$.
 366 Indeed, at $\mathbf{C} = \mathbf{G}$, one obtains $I_4 = I_{40} = \langle \mathbf{G} | \mathbf{A} \rangle = 1$ and the polynomial

$$\mathcal{P}(\mathbf{G}, \mathbf{A}) = \check{\mathcal{P}}(1) = q_0(\mathbf{G}) + \sum_{p=1}^N q_p(\mathbf{G}) \quad (47)$$

367 becomes constant with respect to the structure tensor, thereby rendering the approximation (42) an
 368 identity. Nevertheless, the reliability of (42) deteriorates when \mathbf{C} deviates from \mathbf{G} .

369 To highlight the loss of accuracy of (42) when $\mathbf{C} \neq \mathbf{G}$, let us consider a physically relevant example.
 370 We set $N = 2$, $q_0(\mathbf{C}) = 1$, $q_1(\mathbf{C}) = -2$, and $q_2(\mathbf{C}) = 1$, so that $\mathcal{P}(\mathbf{C}, \mathbf{A})$ takes the form

$$\mathcal{P}(\mathbf{C}, \mathbf{A}) = 1 - 2\langle \mathbf{C} | \mathbf{A} \rangle + \langle \mathbf{C}^{\otimes 2} | \mathbf{A}^{\otimes 2} \rangle = (\langle \mathbf{C} | \mathbf{A} \rangle - 1)^2, \quad (48)$$

371 and we assume that the fibre function \mathcal{F}_1 represents the anisotropic elastic potential of the Holzapfel-
 372 Gasser-Ogden [5] type

$$\hat{\mathcal{F}}_1(\mathbf{C}, \mathbf{A}) = \hat{W}_{1a}(\mathbf{C}, \mathbf{A}) = \frac{1}{2} c_{1a} [\exp(\langle \mathbf{C} | \mathbf{A} \rangle - 1)^2 - 1]. \quad (49)$$

373 In this case, after introducing the auxiliary variable $\eta = (\langle \mathbf{C} | \mathbf{A} \rangle - 1)^2$, the function \mathfrak{f} is identified with

$$\mathfrak{f}(\eta) = \frac{1}{2} c_{1a} [\exp(\eta) - 1]. \quad (50)$$

374 Since \mathfrak{f} can be expanded in Taylor series about $\eta = 0$, we obtain

$$\mathfrak{f}(\eta) = \frac{1}{2} c_{1a} \sum_{n=1}^{+\infty} \frac{\eta^n}{n!}. \quad (51)$$

375 Thus, substituting (51) into (42) yields (for brevity, we omit the dependence of functions on their own
376 arguments)

$$\mathcal{F}_e = \int_{\mathbb{S}^2\mathcal{B}} \Psi \mathfrak{f} = \frac{1}{2} c_{1a} \int_{\mathbb{S}^2\mathcal{B}} \Psi \sum_{n=1}^{+\infty} \frac{\eta^n}{n!} = \frac{1}{2} c_{1a} \sum_{n=1}^{+\infty} \frac{1}{n!} \int_{\mathbb{S}^2\mathcal{B}} \Psi \eta^n. \quad (52)$$

377 At each order $n \geq 1$, we write the integral $\int_{\mathbb{S}^2\mathcal{B}} \Psi \eta^n$ as

$$\int_{\mathbb{S}^2\mathcal{B}} \Psi \eta^n = \left(\int_{\mathbb{S}^2\mathcal{B}} \Psi \eta \right)^n + \mathfrak{R}_n, \quad (53)$$

378 where we refer to \mathfrak{R}_n as to the n -th order residuum of the approximation. Consequently, (52) can be
379 rewritten as

$$\mathcal{F}_e = \frac{1}{2} c_{1a} \sum_{n=1}^{+\infty} \frac{1}{n!} \left(\int_{\mathbb{S}^2\mathcal{B}} \Psi \eta \right)^n + \frac{1}{2} c_{1a} \sum_{n=1}^{+\infty} \frac{1}{n!} \mathfrak{R}_n. \quad (54)$$

380 Since the first term on right-hand-side of (54) is the exponential of the mean value of η , we obtain

$$\begin{aligned} \mathcal{F}_e &= \frac{1}{2} c_{1a} \sum_{n=1}^{+\infty} \frac{1}{n!} \left(\int_{\mathbb{S}^2\mathcal{B}} \Psi \eta \right)^n + \frac{1}{2} c_{1a} \sum_{n=1}^{+\infty} \frac{1}{n!} \mathfrak{R}_n \\ &= \frac{1}{2} c_{1a} \left[\exp \left(\int_{\mathbb{S}^2\mathcal{B}} \Psi \eta \right) - 1 \right] + \frac{1}{2} c_{1a} \sum_{n=1}^{+\infty} \frac{1}{n!} \mathfrak{R}_n \end{aligned} \quad (55)$$

381 We remark that the residuum \mathfrak{R}_n can be computed exactly at any order. Indeed, it holds true that

$$\begin{aligned} \mathfrak{R}_n &= \int_{\mathbb{S}^2\mathcal{B}} \Psi \eta^n - \left(\int_{\mathbb{S}^2\mathcal{B}} \Psi \eta \right)^n \\ &= \sum_{j=0}^{2n} \binom{2n}{j} (-1)^j \langle \mathbf{C}^{\otimes (2n-j)} | \mathbb{H}_{2n-j} \rangle - \left(\langle \mathbf{C}^{\otimes 2} | \mathbb{H}_2 \rangle - 2 \langle \mathbf{C} | \mathbf{H} \rangle + 1 \right)^n. \end{aligned} \quad (56)$$

382 It can be shown, however, that even in the case of an equi-biaxial test (performed on an incompressible
383 material characterised by diagonal matrix representation of \mathbf{C} , $[\mathbf{C}] = \text{diag}\{\lambda^2, \lambda^2, \lambda^{-4}\}$), the residuals
384 may not tend to zero sufficiently fast, even for values of λ sufficiently close to unity. This behaviour
385 contributes to corrupt the reliability of the PARG method and to deteriorate its agreement with the
386 FESD method.

387 We note that, as it happens for the whole $\hat{\mathcal{F}}_1$ in the general case of Equation (8), if \mathcal{P} in Equation
388 (42) is an affine function, i.e., a polynomial of degree one, the PARG method reduces to the GOH
389 method proposed in [6]. The main difference between the PARG method and the GOH method is the
390 level at which the fibre ensemble is approximated. While in the GOH method the averaging integral
391 is performed on the innermost argument, the structure tensor \mathbf{A} , in the PARG method of Equation
392 (42), we take the average of the outermost argument, $\mathcal{P}(\mathbf{C}, \mathbf{A})$, that can be written as a tensor-power
393 polynomial in \mathbf{A} . We remark that, while the GOH method is applicable to any constitutive function,
394 the PARG method is only applicable when the constitutive function is expressible as a function of a
395 tensor-power polynomial in \mathbf{A} .

396 4. Application to Elasticity

397 As an example of application of the integration methods presented in Section 3, we look at the averaged
398 physical quantities that are most often sought for in the mechanics of fibre-reinforced materials and
399 biomechanics of soft tissue: elastic potential and stress. Therefore, our physical quantity \mathcal{F} takes the
400 meaning of elastic potential W in Equation (7), and we write

$$W = \hat{W}(\mathbf{C}, \Psi) = \Phi_0 \hat{W}_0(\mathbf{C}) + \Phi_1 \int_{\mathbb{S}^2\mathcal{B}} \Psi(\mathbf{M}) \hat{W}_1(\mathbf{C}, \mathbf{A}). \quad (57)$$

401 The averaging integral of the fibre potential W_1 is called the *fibre ensemble potential* [17]:

$$W_e = \hat{W}_e(\mathbf{C}, \Psi) = \int_{\mathbb{S}^2\mathcal{B}} \Psi(\mathbf{M}) \hat{W}_1(\mathbf{C}, \mathbf{A}). \quad (58)$$

402 In general, it is possible to attribute some “bulk” isotropic stiffness to the fibres, e.g., by using a fibre
 403 potential \hat{W}_1 given by the sum of an isotropic term and a term depending solely on the anisotropic
 404 invariants I_4 and I_5 [18]. The fibre potential \hat{W}_1 could therefore be written, as a function \check{W}_1 of the
 405 invariants, as

$$\check{W}_1(I_1, I_2, I_3, I_4, I_5) = \check{W}_{1i}(I_1, I_2, I_3) + \check{W}_{1a}(I_4, I_5). \quad (59)$$

406 Furthermore, in those cases in which the contribution of a fibre in direction \mathbf{M} is to be ruled out if
 407 the direction undergoes contraction, i.e., if $I_4 = \mathbf{C} : \mathbf{A} < 1$, it is possible to use the Heaviside step
 408 function \mathcal{H} evaluated at $I_4 - 1$, and write

$$\check{W}_{1a}(I_4, I_5) = \mathcal{H}(I_4 - 1) \check{W}_{1b}(I_4, I_5), \quad (60)$$

409 where \check{W}_{1b} describes the anisotropic behaviour in extension and is called “base” potential. We remark
 410 that, in order to be able to employ the integration methods presented in Section 3, we must renounce
 411 discriminating between fibres in extension (which are unaffected by the Heaviside step function) and
 412 fibres in contraction (which are “killed” by the Heaviside step to reflect the fact that they do not
 413 bear load). Indeed, if we were to use the Heaviside step in the fibre potential as in Equation (59), all
 414 approximating potentials presented in Section 3 would have to be multiplied by the Heaviside step
 415 as well. The Heaviside step with argument $I_4 - 1 = \mathbf{C} : \mathbf{A} - 1$ would rule out the possibility of a
 416 single, direct integration. There are two reasons for this: *a*) it would be in general impossible to know
 417 which fibres undergo contraction *a priori*, and one would have to evaluate this at each increment
 418 of deformation; *b*) the hypotheses of continuity and differentiability necessary for expandability of
 419 functions in Taylor series would be, in general, violated. Therefore, an integration at each increment
 420 of deformation would remain the only available solution method, thus defeating the purpose of the
 421 proposed approximation methods.

422 This means that, in terms of range of applicability to the evaluation of the overall elastic behav-
 423 iour, the methods presented in Section 3 are limited to those cases in which all fibres, or at least
 424 most of the fibres, are in extension. This can be safely said for tissues with fibres lying mostly on a
 425 plane and subjected to tensile plane stress. A typical example is that of blood vessels, which work as
 426 inflated-extended tubes under physiological conditions. Schematically, blood vessels can be represented
 427 as having, at every point, two dominant fibre directions (with some dispersion) mostly contained in
 428 the tangent plane at that point (see, e.g., Figure 1 in [5]).

429 **Remark.** We are aware of the existence of mathematical models in which the collagen fibres contribute
 430 to the tissue’s overall compressive stiffness. It has been recently reported [40] that this is the case, for
 431 example, in aged or diseased intervertebral discs, and it was assumed that the fibres’ contribution to
 432 compressive loads increases with increasing strain magnitude and is influenced by the orientation of
 433 the fibres. Still, to the best of our knowledge and understanding, in articular cartilage (the tissue which
 434 motivated our current study) no correlation of compressive stiffness with collagen content has been
 435 observed [41]. For this reason, we decided to exclude all fibres that are not stretched. Even though
 436 this modelling assumption may turn out to be far from reality in some circumstances, we do not make
 437 it with the purpose of simplifying the calculations. On the contrary, the necessary introduction of the
 438 Heaviside step in the evaluation of the fibre ensemble makes it highly non-linear in a non-differentiable
 439 way, thereby excluding *a priori* the possibility of applying the methods proposed in this work.

440 For our illustrative purposes, let us choose simple forms of the matrix potential \hat{W}_0 , isotropic
 441 fibre potential \hat{W}_{1i} and (base) anisotropic fibre potential \hat{W}_{1b} (such that $\hat{W}_{1a} = \mathcal{H}(I_4 - 1) \hat{W}_{1b}$),

$$\hat{W}_0(\mathbf{C}) = \frac{1}{2} c_0 (I_1(\mathbf{C}) - 3), \quad (61a)$$

$$\hat{W}_{1i}(\mathbf{C}) = \frac{1}{2} c_{1i} (I_1(\mathbf{C}) - 3), \quad (61b)$$

$$\hat{W}_{1b}(\mathbf{C}, \mathbf{A}) = \frac{1}{2} c_{1a} [\exp((\mathbf{C} : \mathbf{A} - 1)^2) - 1], \quad (61c)$$

442 in which c_0 , c_{1i} and c_{1a} are material parameters, and we assume referential volumetric fractions
 443 $\Phi_0 = \Phi_1 = 0.5$. The exponential form of the base anisotropic potential in Equation (61c) has been
 444 chosen because it predicts well the characteristic stress response of soft tissues with collagen fibres
 445 being undulated in the undeformed configuration, with a toe region and a region of increased stiffness
 446 [42]. Moreover, since it consists of the exponential of a polynomial in $I_4 = \mathbf{C} : \mathbf{A}$, it also allows the
 447 use of the PARG method proposed in Section 3.3. Note that, although the invariant I_5 should also
 448 be included in order to obtain a complete transversely isotropic representation (and avoid unphysical
 449 results, see, e.g., [43]), very often I_5 is left out, in order to limit the number of material parameters,
 450 and therefore of experimental tests, needed to characterise the material. In passing, we note that the
 451 form chosen for \hat{W}_1 makes it a particular case of exponential Fung potential [44, 45, 46, 47], which is
 452 the exponential of a quadratic form in the Green-Lagrange strain. Indeed, by using the definition of
 453 Green-Lagrange strain $\mathbf{E} = \frac{1}{2}(\mathbf{C} - \mathbf{G})$, we can write the argument of the exponential in (61c) as a
 454 quadratic form in \mathbf{E} :

$$(\mathbf{C} : \mathbf{A} - 1)^2 = (\mathbf{C} : \mathbf{A} - \mathbf{G} : \mathbf{A})^2 = (2\mathbf{E} : \mathbf{A})^2 = 4 [\mathbf{E} : (\mathbf{A} \otimes \mathbf{A}) : \mathbf{E}]. \quad (62)$$

455 In a Cartesian (material) reference frame with axes \mathbf{E}_1 , \mathbf{E}_2 , \mathbf{E}_3 , we consider a sample of incom-
 456 pressible soft tissue, which undergoes a biaxial tension test in directions \mathbf{E}_1 and \mathbf{E}_2 , with a prescribed
 457 ratio of the nominal strain in direction 2 to the nominal strain in direction 1, i.e.,

$$\zeta = \frac{\lambda_2 - 1}{\lambda_1 - 1}. \quad (63)$$

458 In an isochoric ($J = \det \mathbf{F} = 1$) biaxial test in directions \mathbf{E}_1 and \mathbf{E}_2 , with nominal strain ratio ζ , the
 459 matrix representations of the deformation gradient \mathbf{F} and the right Cauchy-Green deformation \mathbf{C} are

$$[\mathbf{F}] = \text{diag} \left[\lambda, \zeta(\lambda - 1) + 1, \frac{1}{\lambda(\zeta(\lambda - 1) + 1)} \right], \quad (64)$$

$$[\mathbf{C}] = \text{diag} \left[\lambda^2, (\zeta(\lambda - 1) + 1)^2, \frac{1}{\lambda^2(\zeta(\lambda - 1) + 1)^2} \right], \quad (65)$$

460 so that $\zeta = 1$ describes an equi-biaxial test, for which $[\mathbf{F}] = \text{diag}[\lambda, \lambda, \lambda^{-2}]$ and $[\mathbf{C}] = \text{diag}[\lambda^2, \lambda^2, \lambda^{-4}]$,
 461 $0 < \zeta < 1$ means that direction \mathbf{E}_1 is being stretched more than direction \mathbf{E}_2 , and $\zeta > 1$ vice versa.

462 We assume that the fibres are oriented according to a transversely isotropic von Mises distribution
 463 (see, e.g., [6, 20, 48]),

$$\varrho(\Theta) = \frac{1}{\pi} \sqrt{\frac{b}{2\pi}} \frac{\exp[b(\cos(2\Theta) + 1)]}{\text{erfi}(\sqrt{2b})}, \quad (66)$$

464 where Θ is the angle between the generic direction \mathbf{M} and the axis of transverse isotropy \mathbf{M}_0 , $\text{erf}(x)$
 465 and $\text{erfi}(x) = -i \text{erf}(ix)$ denote the error function at x and the imaginary error function at x , respec-
 466 tively [49], and b is called concentration parameter. In the form reported in Equation (66), the von
 467 Mises distribution can accommodate both positive and negative values of the concentration parameter
 468 [50, 48, 19]. The limit $b \rightarrow +\infty$ describes fibres all aligned in the direction \mathbf{M}_0 of the axis of symmetry,
 469 the limit $b \rightarrow 0$ represents isotropy, and the limit $b \rightarrow -\infty$ describes fibres all lying on the transverse
 470 plane, which is, by definition, orthogonal to the direction of the axis of symmetry \mathbf{M}_0 . For simplicity,
 471 we assume that the axis of symmetry \mathbf{M}_0 coincides with the direction \mathbf{E}_1 of axis 1 of the biaxial test
 472 (Figure 1).

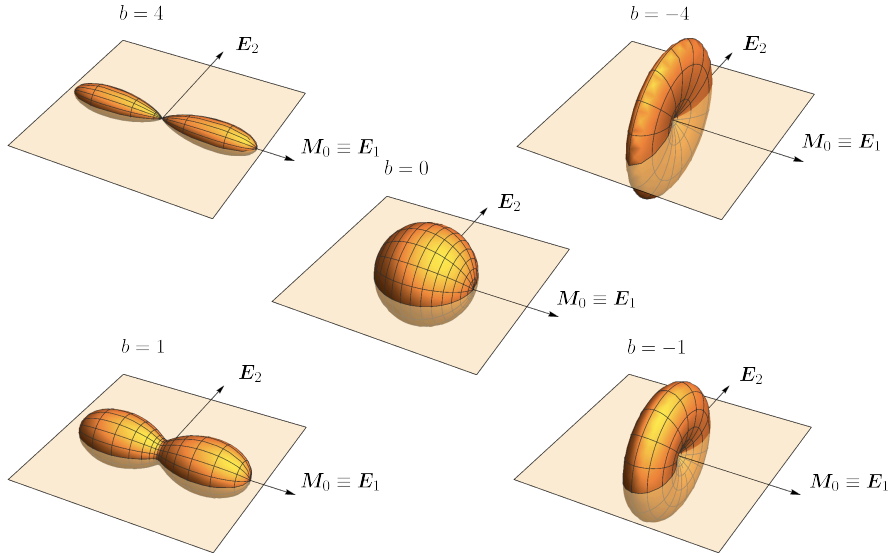


FIGURE 1. Fibre arrangement for the samples undergoing biaxial test in the plane of directions \mathbf{E}_1 and \mathbf{E}_2 . The orientation of the fibres follows a von Mises distribution with axis of symmetry \mathbf{M}_0 parallel to \mathbf{E}_1 . The cases of $b = 4$ (fibres mostly aligned in the direction of symmetry), $b = 1$, $b = 0$ (fibres isotropically distributed), $b = -1$ and $b = -4$ (fibres mostly lying on the transverse plane) are shown as an example.

473 The approximated integration methods proposed in Section 3 are applied to the calculation of
 474 the ensemble potential \hat{W}_e with the provision that, even if the fibres are modelled as extension-only,
 475 i.e., $\hat{W}_{1a} = \mathcal{H}(I_4 - 1)\hat{W}_{1b}$, the approximation is made with $\hat{W}_{1a} \equiv \hat{W}_{1b}$. Indeed, as noted above, we
 476 *must* renounce to excluding the fibres in contraction when employing our approximation methods.
 477 The three proposed methods are implemented with the assumptions outlined below:

- 478 1. INEX: the expansion is performed about $\bar{I}_{40} = 1$ as outlined in Section 3.1, and is truncated at
 479 order 6, which, in contrast with what happens with the structure tensor expansion STEX, is still
 480 computationally manageable;
- 481 2. STEX: the expansion is performed about the structure tensor $\mathbf{A}_0 = \mathbf{M}_0 \otimes \mathbf{M}_0$ of the direction
 482 $\mathbf{M}_0 \equiv \mathbf{E}_1$ of the axis of symmetry of the potential; the expansion is truncated at order 4, which
 483 is the maximum order of expansion that the computational resources in our hands allowed;
- 484 3. PARG: the outermost argument of polynomial form in the fibre potential \hat{W}_1 of Equation (61c)
 485 is given by $(\mathbf{C} : \mathbf{A} - 1)^2$, the directional average of which is evaluated.

486 The three proposed methods are compared against:

- 487 4. GOH: replacement of the structure tensor \mathbf{A} in Equation (61c) with the directional average \mathbf{H}
 488 of Equation (18) [6];
- 489 5. FESD: integration of the fibre ensemble, at each increment of deformation, by means of the
 490 method of the spherical t -designs; note that all fibres, in extension and contraction, are taken
 491 into account, i.e., as in the three proposed methods, we consider $\hat{W}_{1a} \equiv \hat{W}_{1b}$;
- 492 6. FESDH: integration of the fibre ensemble at the each increment of deformation, as originally
 493 introduced in [20] for the elastic properties, i.e., with the fibre potential $\hat{W}_{1a} = \mathcal{H}(I_4 - 1)\hat{W}_{1b}$,
 494 that “kills” the fibres in contraction; this is done to verify under which conditions “sparing” the
 495 fibres in contraction is an acceptable approximation.

496 The method for the evaluation of the stresses is provided in Appendix E. The values of the elastic
 497 potential W and the total Cauchy stresses σ^{11} and σ^{22} are plotted as a function of the stretch λ under
 498 the deformation described by Equation (65), and are normalised with respect to the material parameter

499 c_0 of Equation (61a), while c_{1i} and c_{1a} are assumed to have the values $0.5 c_0$ and $5 c_0$ respectively. At
 500 a given value of the strain ratio ζ , a set of three plots (W , σ^{11} and σ^{22}) is produced for each value
 501 of the concentration parameter b equal to 4 (strong alignment in the direction of symmetry of the
 502 probability distribution), 1 (weak alignment), 0 (isotropic distribution), -1 (weak alignment on the
 503 transverse plane), -4 (strong alignment). Figure 2 reports the plots obtained for $\zeta = 1$ (equi-biaxial
 504 test), Figure 3 for $\zeta = 0.5$ (direction \mathbf{E}_1 stretched more than direction \mathbf{E}_2) and Figure 4 for $\zeta = 2$
 505 (direction \mathbf{E}_2 stretched more than direction \mathbf{E}_1). All calculations were performed with *Mathematica*
 506 (Wolfram Research, Champaign, Illinois, USA).

507 We note (Figure 1) that the fibre distribution with negative values of the concentration parameter
 508 b is quite unrealistic: in a quasi-two-dimensional sample of a real soft tissue, very few fibres would
 509 be oriented out-of-plane. We chose to keep this distribution, particularly for the quite extreme case
 510 of $b = -4$, because most of the fibres are oriented out-of-plane, and therefore undergo contraction.
 511 This offers a way to verify what discrepancy the fibres in contraction cause between the results of the
 512 FESD calculation that does not exclude them and those of the FESDH calculation that does exclude
 513 them.

514 5. Results

515 The FESDH method, including the Heaviside function in order to “kill” the fibres in contraction, is
 516 regarded as the “correct” computation, in so far as it rigorously follows the rule of mixtures as in
 517 Equations (7) and (57). For the tested values of the concentration parameter b and the strain ratio
 518 ζ , the FESD that does not discriminate between fibres in extension and contraction gives very close
 519 results to the “correct” FESDH method, except for some discrepancy, mainly in the potential, for the
 520 case of large negative b . A discrepancy between FESD and FESDH is expected as, for large negative
 521 b , the orientation of a quite large fraction of the fibres is close to the \mathbf{E}_3 (out of plane) direction, and
 522 these fibres are therefore in contraction. However, the discrepancy is much smaller than expected (see,
 523 e.g., the plots for $b = -1$ and $b = -4$ in Figure 3).

524 Among all tested methods, the INEX method is systematically the one that gives the results
 525 closest to those of FESDH/FESD for all values of b in the equi-biaxial case (Figure 2), almost always
 526 in the case of $\zeta = 0.5$, except in a few cases in which it is slightly outperformed by the PARG method
 527 and the GOH method (e.g., potential and stresses for $b = 4$, Figure 3). For $\zeta = 2$, while the INEX
 528 method is generally the second closest to the spherical designs method (after the STEx method, as
 529 mentioned below), the fit is not as good as in the cases of $\zeta = 1$ and $\zeta = 0.5$.

530 The STEx method is by far the most inappropriate. As expected, it works best when the proba-
 531 bility Ψ is peaked around the direction \mathbf{M}_0 about which the expansion is performed. For the considered
 532 von Mises probability, this situation corresponds to values of the concentration parameter b greater
 533 than zero. Indeed, for the fairly large value $b = 4$, it is very close to the FESDH/FESD method.
 534 However, even for $b = 4$, it fails to describe a physically correct behaviour for the stress in direction
 535 2, when $\zeta = 0.5$ (Figure 3). The results become generally disastrous for lower values of b , with several
 536 occurrences of unphysical behaviour (i.e., decreasing stress in direction 2 for increasing strain), al-
 537 though in some cases (e.g., particularly for $\zeta = 2$, Figure 4) the STEx method evaluates the potential
 538 very accurately, even for small or negative b .

539 The PARG method turned out to be a fairly reasonable approximation of the FESDH/FESD
 540 method. For the equi-biaxial test (Figure 2) and for $\zeta = 2$ (Figure 4), it is more accurate for positive
 541 values of b . However, this trend is reversed for $\zeta = 0.5$ (Figure 3), i.e., the PARG works better for
 542 negative values of b . In general, for given b and ζ , the values of the potential and the stresses yielded by
 543 the PARG method lie between those of the INEX and the GOH methods, with a few exceptions (e.g.,
 544 $b = 4$ in the equi-biaxial test and $b = 4, -4$ for $\zeta = 0.5$) where the PARG method is the closest to the
 545 FESDH/FESD method. For all tested conditions, the PARG method is closer to the FESDH/FESD
 546 method than the GOH method is.

547 The GOH method has a good agreement with the FESDH/FESD method for large positive values
 548 of the concentration parameter b . However, for $b = 0$ (isotropic distribution) and negative values of
 549 b , the behaviour of the GOH method deviates quite substantially from that of the FESDH/FESD
 550 method. For the tested values of b and ζ , the behaviour of the GOH method is easily predictable, in
 551 the sense that, for a given ζ , a higher value of b necessarily means a behaviour closer to FESDH/FESD,
 552 and there seems to be no exceptions.

553 To give an idea about the computational time for each method, we show in Table 1 the time
 554 required to produce the curves for the equi-biaxial test reported in Figure 2 for $b = 4$. In order to
 555 examine quantitatively the accuracy of the proposed methods, we provide in Figures 5a and 5b the
 556 curves describing, for two different values of the concentration parameter b , the absolute error of the
 557 elastic potential W , computed for $\lambda \in [1.0, 1.6]$ by regarding the FESDH method as the reference
 558 one, i.e., $\mathcal{E}_M := |W_M - W_{\text{FESDH}}|$, with $M \in \{\text{STEX}, \text{INEX}, \text{PARG}, \text{GOH}, \text{FESD}\}$. The thin, black
 559 lines corresponding to the values of the absolute error 0.05 for $b = 4$, and 0.1 for $b = -4$ define a
 560 threshold that identifies, for each value of the concentration parameter, a maximal range of validity,
 561 i.e., the maximal subset of the stretch interval $[1.0, 1.6]$ within which the absolute error is assumed
 562 to be acceptable. Furthermore, for a given value of λ belonging to this range, i.e., $\lambda = 1.3$, Table 2
 563 and 3 report the values of the relative error of the elastic potential and the stress σ^{11} for varying
 564 concentration parameter b . In doing this, we take the FESDH method as the term of comparison.

565 Clearly, the results obtained by using the FESD approach are by far the closest to the ones
 566 determined by FESDH. This is because the two procedures differ from each other only by the presence
 567 of the Heaviside step function. Thus, for situations in which almost all fibres are stretched, there is
 568 virtually no difference between FESD and FESDH. In contrast, when there is a substantial fraction of
 569 fibres that are not stretched, the results obtained by employing the FESD deviate from those predicted
 570 by the FESDH. Specifically, both the amplitude and the sense of the deviations depend on the stretch
 571 λ , concentration parameter b , and deformation mode ζ . For example, the FESD overestimates the
 572 values of W/c_0 for $\zeta = 1$ and $b = -4$ (cf. Figure 2), while it underestimates them for $\zeta = 2$ and $b = -4$
 573 (cf. Figure 4). Looking at Table 2, we also notice that, in contrast to what happens for all other
 574 methods, the relative error pertaining to INEX decreases with decreasing b , i.e., when the fibres tend
 575 to lie transversely to the symmetry axis. We argue that this result is related to the fact that the INEX
 576 method does not select any particular structure tensor for the Taylor expansion formula approximating
 577 the elastic potential. On the contrary, since the STEX method necessitates to specify the structure
 578 tensor around which the Taylor expansion formula is constructed, it produces a comparatively small
 579 absolute error (cf. Figure 5a) when the fibres are concentrated around a given direction ($b = 4$), while
 580 its accuracy deteriorates for decreasing b , i.e., when the fibres tend to deviate from that direction.

581 We notice that, for $b = 4$, the INEX and PARG approximations are the closest to FESDH/FESD.
 582 For the case of PARG, this may be due to the fact that this method does not substitute $\hat{\mathcal{F}}_1$ with its
 583 Taylor polynomial but, rather, it calculates an *exact* average of the polynomial argument of the fibre
 584 constitutive function. Thus, the more the fibres are peaked around a given direction, the more accurate
 585 the PARG method becomes. Looking at the columns of Tables 2 and 3 relative to the INEX and PARG
 586 methods, we notice that the choice of the “optimal” approximation criterion is quite problem-dependent
 587 (i.e., it depends on b). Consequently, there could be cases (e.g., in inhomogeneous problems, or if b
 588 changes in time due to some sort of tissue remodelling) in which the approximation method has to
 589 be chosen adaptively, thereby switching from one to the other in order to minimise the error. For
 590 completeness, we mention that the relative errors associated with the stress σ^{11} are not monotonic
 591 functions of b for the FESD and the PARG methods. A plausible explanation for this behaviour could
 592 be their capability of resolving the fibre orientation with increasing dispersion (i.e., with $b \rightarrow -\infty$).

593 All the methods belonging to the class of approximations not calling for step-by-step integrations
 594 (such as the algorithms based on the spherical designs) fail to be accurate after some “threshold” value
 595 of the stretch that depends on the deformation mode (biaxial, equi-biaxial, etc.) as well as on the
 596 concentration parameter associated with the chosen probability density distribution.

597 As is visible in the plots of the components of Cauchy stress, the main influence on the mono-
 598 tonicity and convexity of the curves is given by the interplay between the concentration parameter, b ,
 599 which characterises the von Mises distribution, and the parameter ζ , which defines the deformation
 600 mode. In particular, for $\zeta = 1$ and $\zeta = 0.5$, the stress curves lose convexity with decreasing b . Indeed,
 601 when the deformation along the symmetry axis is greater than, or equal to, the deformation in the
 602 transverse plane, on which the fibres tend to lie for decreasing b , the STEX method is the one that
 603 deviates the most from the FESDH predictions, thereby introducing unphysical stiffnesses (cf. e.g.,
 604 Figures 2 and 3).

605 Moreover, a computation of the stress, e.g., σ^{11} , shows that the summand of σ^{11} responsible
 606 for the concavity in the stress curves is given by the Lagrange multiplier introduced to account for
 607 the incompressibility constraint. To show that this is actually the case, we take as example the stress
 608 approximated by means of the INEX method. Hereafter, for ease of demonstration, we write its
 609 expression only for the Taylor expansion of the elastic potential up to the second order. In the figures,
 610 however, we show also the stress for the case of an expansion up to the sixth order. By using the
 611 elastic potential (57), along with (61a)–(61c) and arresting the Taylor expansion of $\hat{W}_1(\mathbf{C}, \mathbf{A})$ at the
 612 order $n = 2$, the approximated expression of the constitutive part of the second Piola-Kirchhoff stress
 613 tensor reads

$$\mathbf{S}_c^{\text{app}} := 2 \frac{\partial \hat{W}}{\partial \mathbf{C}}(\mathbf{C}) = \Phi_0 c_0 \mathbf{G}^{-1} + \Phi_1 c_{1i} \mathbf{G}^{-1} + \mathbf{S}_{1a}^{\text{app}}, \quad (67)$$

614 where (cf. (98))

$$\mathbf{S}_{1a}^{\text{app}} = 2\Phi_1 c_{1a} [\mathbb{H}_2 : \mathbf{C} - \mathbb{H}_1]. \quad (68)$$

615 Because of the imposed incompressibility, the overall second Piola-Kirchhoff stress tensor is given by
 616 $\mathbf{S}^{\text{app}} = -p\mathbf{C}^{-1} + \mathbf{S}_c^{\text{app}}$, where p is the Lagrange multiplier (*not* coinciding with the pressure in the
 617 present treatment) associated with the incompressibility constraint. Accordingly, for an equi-biaxial
 618 test (i.e., when $[\mathbf{C}] = \text{diag}\{\lambda^2, \lambda^2, \lambda^{-4}\}$), the component σ^{11} of the Cauchy stress tensor becomes

$$\sigma^{11} = -p + (\Phi_0 c_0 + \Phi_1 c_{1i}) \lambda^4 + \sigma_{1a}^{11}, \quad (69)$$

619 with $\sigma_c^{11} := (\Phi_0 c_0 + \Phi_1 c_{1i}) \lambda^4 + \sigma_{1a}^{11}$ being the constitutive part of σ^{11} and

$$\sigma_{1a}^{11} = 2\Phi_1 c_{1a} [(\mathbb{H}_2)^{1111} \lambda^4 + (\mathbb{H}_2)^{1122} \lambda^4 + (\mathbb{H}_2)^{1133} \frac{1}{\lambda^2} - (\mathbb{H}_1)^{11} \lambda^2]. \quad (70)$$

620 Plotting σ^{11} versus λ shows that σ_c^{11} is a convex function of λ , whereas the negative of the Lagrange
 621 multiplier, $-p$, is a concave function λ . Since σ_c^{11} grows almost linearly for values of λ close to unity,
 622 the composition $\sigma^{11} = -p + \sigma_c^{11}$ turns out to be non-convex. This is depicted in Figures 6a and 6b,
 623 where the effect of raising the order of the approximation is testified by the increasing curvature, for
 large enough values of λ of the constitutive part of stress.

TABLE 1. Computational time [s] for graphs at $\zeta = 1$ and $b = 4$ and stretch range $\lambda \in [1.0, 1.6]$; time increment in FESD and FESDH is 40 ms.

Quantity	STEX	INEX	PARG	GOH	FESD	FESDH
elastic potential W	0.66	0.06	0.05	0.06	1.66	2.81
stress σ^{11}	0.78	0.44	0.08	0.14	25.20	38.80
stress σ^{22}	0.19	0.55	0.08	0.06	25.34	38.17

624

625 6. Summary and Discussion

626 In a biological tissue (or industrial material) with a statistical distribution of reinforcing fibres, the
 627 effect of the fibres on the overall constitutive function $\hat{\mathcal{F}}$ of a given physical quantity can be obtained

TABLE 2. Relative error [%] for the elastic potential W , in the equi-biaxial test ($\zeta = 1$) and at $\lambda = 1.3$.

b	FESD	INEX	STEX	PARG	GOH
4	0.06	0.04	1.30	1.13	4.85
1	3.87	4.63	45.35	1.26	26.92
0	9.20	10.26	102.85	6.44	14.86
-1	14.99	16.45	163.98	12.49	29.02
-4	23.02	25.99	250.77	21.95	39.35

TABLE 3. Relative error [%] for the stress σ^{11} , in the equi-biaxial test ($\zeta = 1$) and at $\lambda = 1.3$.

b	FESD	INEX	STEX	PARG	GOH
4	0.0007	0.7728	3.5272	2.9521	6.9328
1	0.7915	1.2773	181.0450	6.5662	34.0420
0	3.0387	3.8109	552.9186	4.2988	41.0398
-1	7.6397	8.7854	1205.4554	2.3712	35.4135
-4	20.4896	22.8115	2664.3860	19.3050	13.5467

628 by integrating the fibre constitutive function $\hat{\mathcal{F}}_1$, weighted by an orientation probability distribution,
629 over the set of all directions in space (cf. Equation (7)). The resulting integral, called fibre ensemble
630 $\hat{\mathcal{F}}_e$ in this work (cf. Equation (8)), can in general only be evaluated numerically at each increment
631 of deformation, since the deformation (usually represented by the right Cauchy-Green deformation
632 tensor \mathbf{C}) cannot be factorised out of the integral sign, except in the case in which $\hat{\mathcal{F}}_1$ is expressed as a
633 tensor-power polynomial in the structure tensor \mathbf{A} [19]. Even though the numerical integration of $\hat{\mathcal{F}}_e$ is
634 flexible and can be made very accurate, it is sometimes computationally expensive. Indeed, especially
635 in time-dependent nonlinear problems, it has to be “called” at each time-step and at each iteration of
636 some nonlinear solver, thereby increasing computational costs. With the aim of containing these costs,
637 we exploited polynomials to achieve a single, direct integration of a given fibre constitutive function
638 $\hat{\mathcal{F}}_1$, and thus an approximation of the corresponding fibre ensemble $\hat{\mathcal{F}}_e$. We elaborated three methods:
639 a Taylor expansion in the transversely isotropic invariants (INEX method), which we presented in the
640 case of functions of the fourth invariant I_4 alone, but which can be seamlessly extended to functions
641 including also the fifth invariant, I_5 ; a Taylor expansion in the structure tensor \mathbf{A} about a given
642 value \mathbf{A}_0 corresponding to a direction \mathbf{M}_0 (STEX method); and, for the case of fibre constitutive
643 functions $\hat{\mathcal{F}}_1$ expressed as some function of a polynomial $\mathcal{P}(\mathbf{C}, \mathbf{A})$, the replacement of $\mathcal{P}(\mathbf{C}, \mathbf{A})$ with
644 its directional average (PARG method). The latter method is similar to the GOH method proposed
645 in [6]. We emphasise that our methods are not meant to replace the step-by-step integration, which
646 is considered to be the most accurate method to represent a constitutive function expressed by the
647 rule of mixtures, and was regarded as term of comparison to test the accuracy of our approximations.
648 Rather, our methods aim to offer alternative options to step-by-step integration schemes, such as the
649 FESD and the FESDH, since the direct integration of constitutive functions can be performed *before*
650 discretising the system in time and before starting any iterative scheme for solving nonlinear problems.

651 We chose to test the proposed methods for the case of the elastic potential and the associated
652 stress. We compared the proposed methods to the “exact” integration, performed at each increment
653 of deformation by means of the method of the spherical designs [21, 34, 20], which we have called here
654 FESD method, as well as to the GOH method [6]. A calculation including the Heaviside function was
655 made with the method of the spherical designs (FESDH method) in order to eliminate the contribution
656 of the fibres in contraction and to estimate in which conditions counting also the fibres undergoing
657 contraction is acceptable.

658 As mentioned in Section 5, for most of the tested conditions, the INEX method (expansion in the
 659 invariants) was the closest to the “rigorous” integration performed with FESDH/FESD method (fibre
 660 ensemble evaluated by means of the method of the spherical designs, with or without the Heaviside
 661 function to eliminate the fibres in contraction). What really distinguishes the INEX method from the
 662 other ones is that its accuracy is weakly dependent on the distribution of the fibres (concentration
 663 parameter b). Moreover, one could improve the accuracy of the approximation by simply computing a
 664 higher-order expansion. In contrast, the accuracy of the other tested methods shows a clear dependence
 665 on the distribution of the fibres, i.e., their accuracy is higher for high values of b and decreases, often
 666 sensibly, as b becomes negative.

667 In conclusion, when implementing the fibre ensemble (Equation (8)) arising from the rule of
 668 mixtures into Finite Elements, the method of Taylor expansion in the invariants (INEX) constitutes a
 669 valid, computationally inexpensive, direct integration method, alternative to programming a complex
 670 user subroutine that employs the method of the spherical designs to perform the directional averages
 671 at each increment of deformation. The integrals \mathbb{H}_p needed in the INEX method (Equations (27) and
 672 (35)) can be evaluated directly (Equation (13)) with a commercially available calculation package
 673 such as *Mathematica* (Wolfram Research, Champaign, Illinois, USA), and then exported into a much
 674 simpler user subroutine to be used in the Finite Element code. In fact, once the highest order $2n$ of
 675 the expansion is set, one can simply calculate the corresponding tensor \mathbb{H}_n , and then obtain all tensors
 676 \mathbb{H}_p of lower order $2 \leq 2p < 2n$ by contracting any $n - p$ pairs of indices [31]. Moreover, for the case
 677 of the von Mises distribution, which is determined univocally by the concentration parameter b , the
 678 tensors \mathbb{H}_p can be exported as functions of b , which has the obvious advantage of providing a function
 679 rather than an array of values. It is in our future plans to develop similar methods for fibre-reinforced
 680 biological tissues seen as higher-gradient materials (see, e.g., [51, 52, 53]).

681 Acknowledgements

682 We would like to thank Lorenzo Tentarelli (DISMA, Politecnico di Torino) for useful discussions.
 683 This work was supported in part by Alberta Innovates - Technology Futures (Canada), through the
 684 AITF New Faculty Programme [SF], Alberta Innovates - Health Solutions (Canada), through the
 685 Sustainability Programme [SF], the Natural Sciences and Engineering Research Council of Canada,
 686 through the NSERC Discovery Programme [SF], and by the *Politecnico di Torino* and the *Fondazione*
 687 *Cassa di Risparmio di Torino* in the context of the funding campaign “*La Ricerca dei Talenti*” (HR
 688 Excellence in Research) [AG].

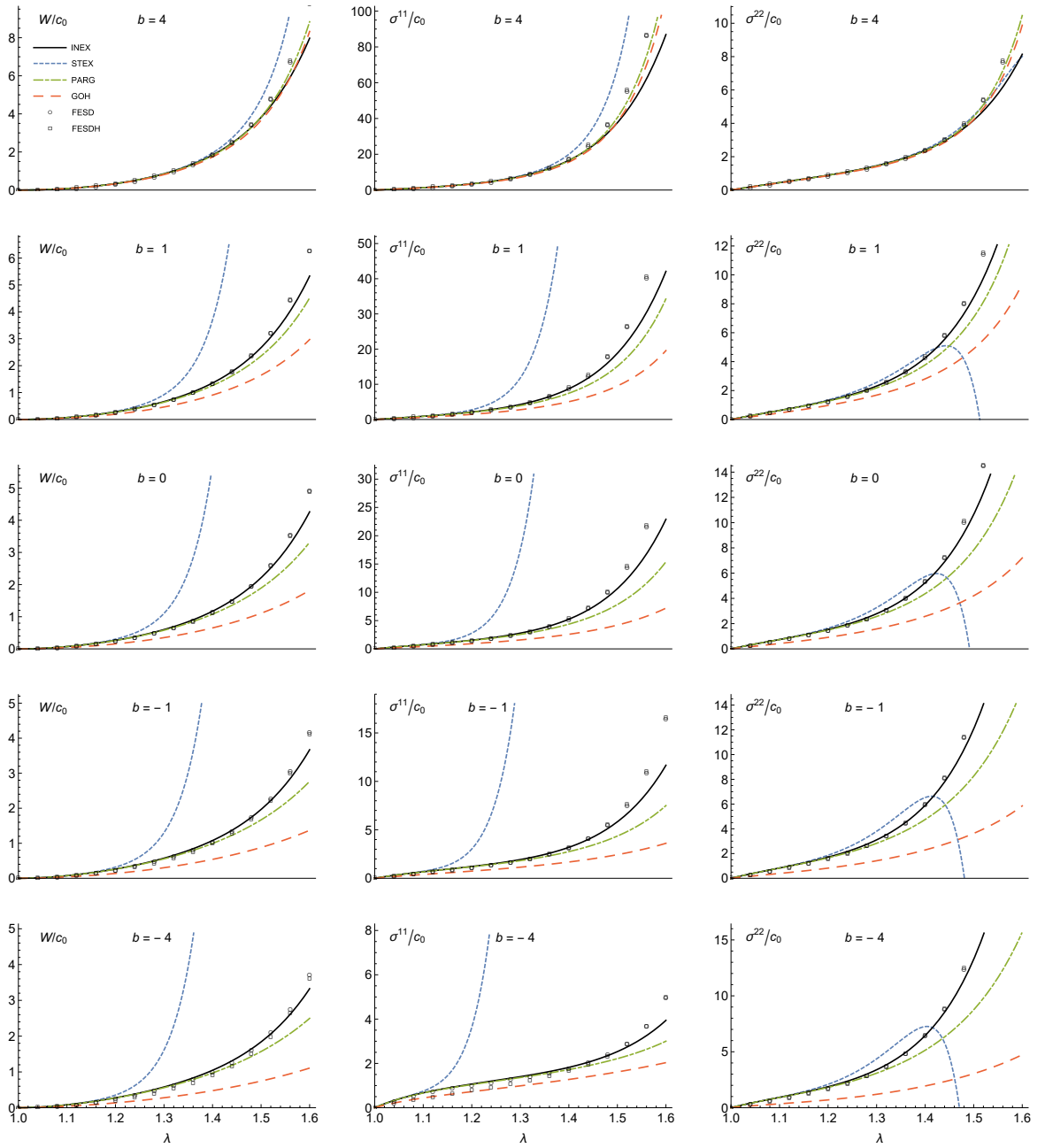


FIGURE 2. Elastic potential and stress for the equi-biaxial test ($\zeta = 1$)

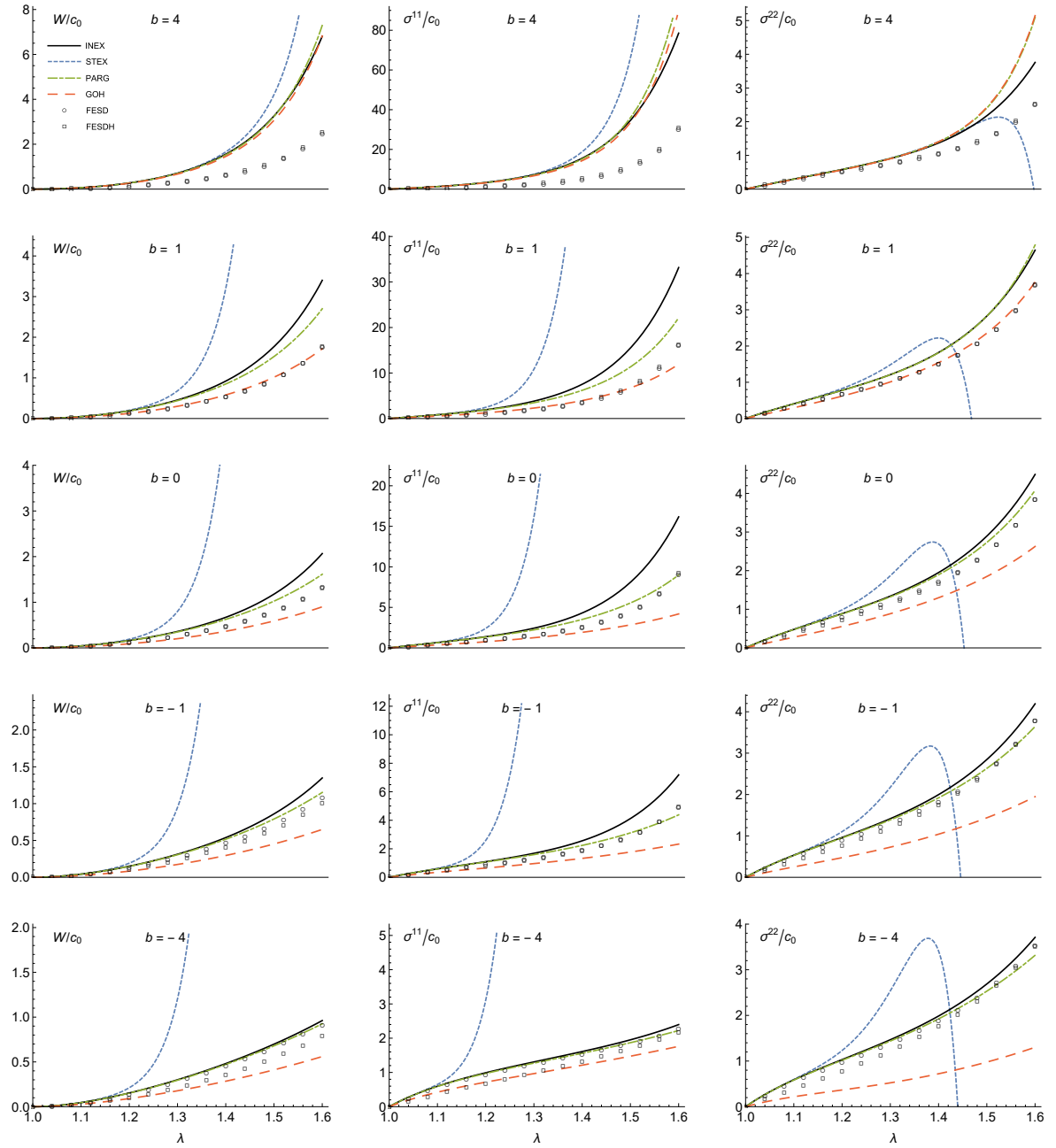


FIGURE 3. Elastic potential and stress for a biaxial test with $\zeta = 0.5$

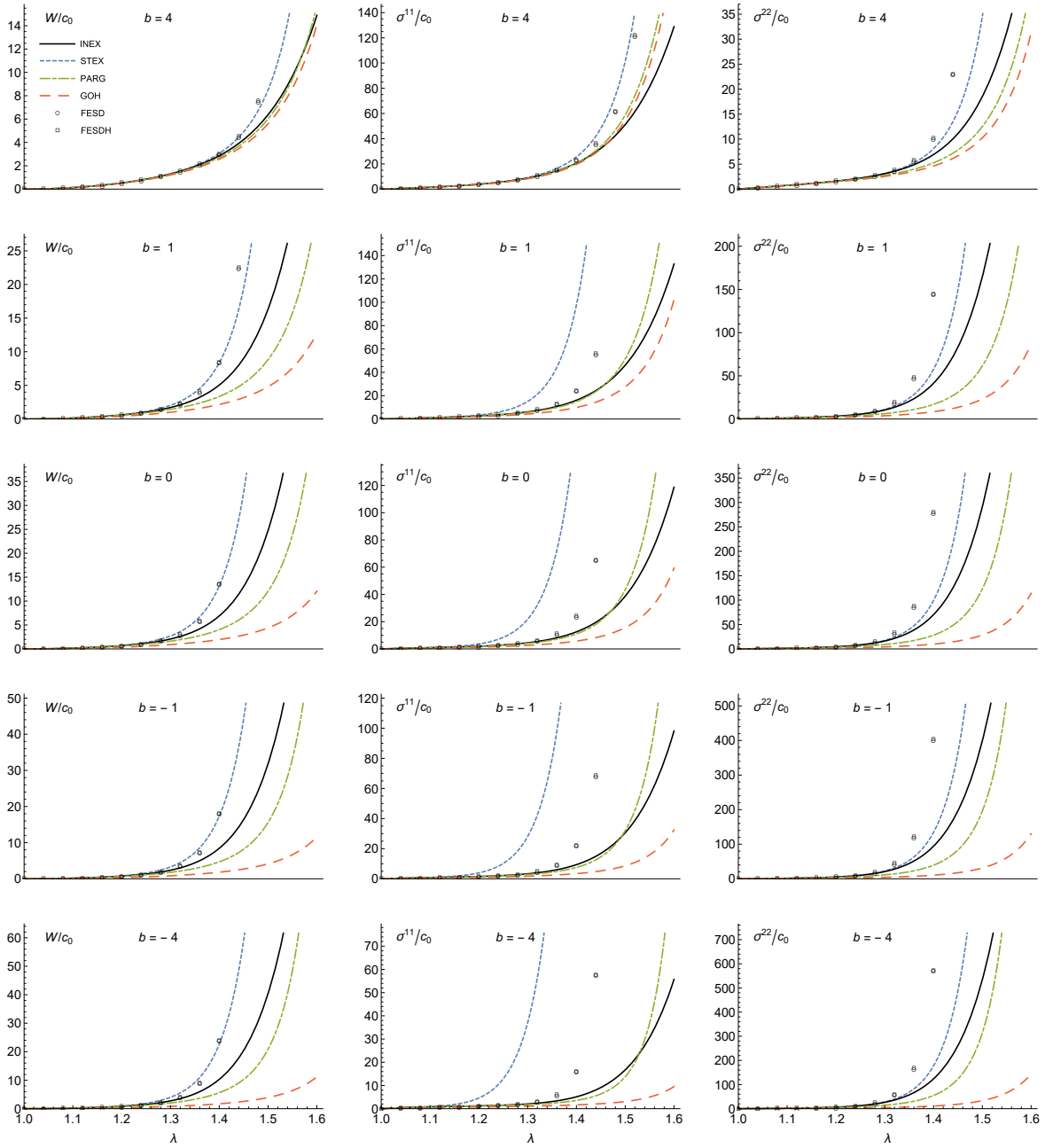


FIGURE 4. Elastic potential and stress for a biaxial test with $\zeta = 2$

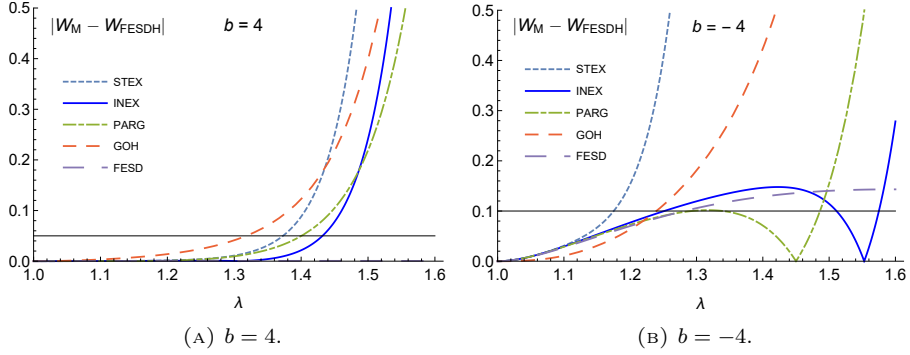


FIGURE 5. Absolute error $|W_M - W_{\text{FESDH}}|$ of the elastic potential W , with $M \in \{\text{STEX, INEX, PARG, GOH, FESD}\}$, for two different values of the concentration parameter, $b = 4$ and $b = -4$.

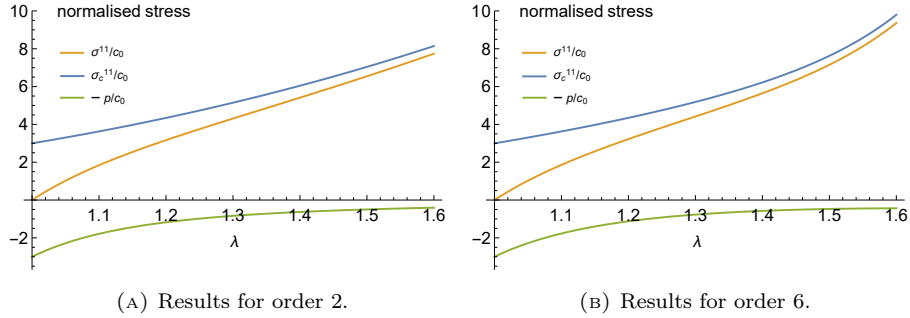


FIGURE 6. Normalised stresses and pressure for the INEX method (orders 2 and 6).

689 Appendix A. Continuum Mechanics Notation and Definitions

690 The deformation χ maps material points $X = (X^1, X^2, X^3)$ in the reference configuration \mathcal{B} into
 691 spatial points $x = (x^1, x^2, x^3)$ in the physical space \mathcal{S} . The deformation gradient \mathbf{F} has components
 692 $F^a_A = \chi^a_{,A}$ and pushes-forward material vectors \mathbf{W} with components W^A into spatial vectors \mathbf{FW}
 693 with components $F^a_A W^A$. The inverse \mathbf{F}^{-1} pulls-back spatial vectors \mathbf{w} with components w^a into
 694 material vectors $\mathbf{F}^{-1}\mathbf{w}$ with components $(\mathbf{F}^{-1})^A_a w^a$. The transpose \mathbf{F}^T pulls-back spatial covectors $\boldsymbol{\pi}$
 695 with components π_a into material covectors $\mathbf{F}^T\boldsymbol{\pi}$ with components $(\mathbf{F}^T)_A^a \pi_a = F^a_A \pi_a$. The inverse
 696 transpose \mathbf{F}^{-T} pushes-forward material covectors $\boldsymbol{\Pi}$ with components Π_A into spatial covectors $\mathbf{F}^{-T}\boldsymbol{\Pi}$
 697 with components $(\mathbf{F}^{-T})_a^A \Pi_A = (\mathbf{F}^{-1})^A_a \Pi_A$. The determinant $J = \det \mathbf{F}$ is called volume ratio and
 698 measures volumetric deformation.

699 The reference configuration \mathcal{B} and the physical space \mathcal{S} are equipped with metric tensors \mathbf{G}
 700 and \mathbf{g} , respectively, which define the scalar products of material and spatial vectors as $\langle \mathbf{W}, \mathbf{Y} \rangle =$
 701 $\mathbf{W} \cdot \mathbf{Y} = \mathbf{W} \mathbf{G} \mathbf{Y} = W^A G_{AB} Y^B$ and $\langle \mathbf{w}, \mathbf{y} \rangle = \mathbf{w} \cdot \mathbf{y} = \mathbf{w} \mathbf{g} \mathbf{y} = w^a g_{ab} y^b$, respectively. The pull-back of
 702 the spatial metric \mathbf{g} is the right Cauchy-Green deformation tensor $\mathbf{C} = \mathbf{F}^T \mathbf{g} \mathbf{F} = \mathbf{F}^T \cdot \mathbf{F}$, with com-
 703 ponents $(\mathbf{F}^T)_A^a g_{ab} F^b_B = F^a_A g_{ab} F^b_B$. The pull-back of the inverse spatial metric \mathbf{g}^{-1} is the Piola
 704 deformation tensor $\mathbf{B} = \mathbf{F}^{-1} \mathbf{g}^{-1} \mathbf{F}^{-T} = \mathbf{F}^{-1} \cdot \mathbf{F}^{-T} = \mathbf{C}^{-1}$, with components $(\mathbf{F}^{-1})^A_a g^{ab} (\mathbf{F}^{-T})_b^B =$
 705 $(\mathbf{F}^{-1})^A_a g^{ab} (\mathbf{F}^{-1})^B_b$. The difference between the *pulled-back material metric* \mathbf{C} and the natural ma-
 706 terial metric \mathbf{G} , normalised by the coefficient $1/2$, is the Green-Lagrange strain $\mathbf{E} = \frac{1}{2}(\mathbf{C} - \mathbf{G})$.

707 Appendix B. Invariants of the Deformation

708 Isotropy is the material symmetry defined as the invariance of a given physical quantity with respect
709 to the whole group of rotations [54]. For an isotropic material, the three scalar invariants of the
710 deformation are

$$I_1 = \text{tr}(\mathbf{C}) = \mathbf{G}^{-1} : \mathbf{C}, \quad (71a)$$

$$I_2 = \frac{1}{2} [(\text{tr}(\mathbf{C}))^2 - \text{tr}(\mathbf{C}^2)], \quad (71b)$$

$$I_3 = \det(\mathbf{C}). \quad (71c)$$

711 Given a vector \mathbf{M} , belonging to the material (or referential) unit sphere $\mathbb{S}^2\mathcal{B} = \{\mathbf{M} : \|\mathbf{M}\| = 1\}$,
712 transverse isotropy with respect to the direction \mathbf{M} is defined as the invariance under arbitrary
713 rotations about \mathbf{M} . When the material properties do not depend on the sense of \mathbf{M} , it is possible to
714 introduce the structure tensor $\mathbf{A} = \mathbf{M} \otimes \mathbf{M}$, which is invariant for inversions of \mathbf{M} , i.e., transformations
715 of the type $\mathbf{M} \mapsto -\mathbf{M}$. For the case of transverse isotropy, two additional invariants are defined as a
716 function of the structure tensor \mathbf{A} [55]:

$$I_4 = \mathbf{C} : \mathbf{A} = \mathbf{M} \mathbf{C} \mathbf{M} = (\mathbf{F} \mathbf{M}) \cdot (\mathbf{F} \mathbf{M}) = \lambda_{\mathbf{M}}^2, \quad (72a)$$

$$I_5 = \mathbf{C}^2 : \mathbf{A}, \quad (72b)$$

717 where $\lambda_{\mathbf{M}}^2$ is the square of the stretch in direction \mathbf{M} . By enforcing the volumetric-distortional decom-
718 position of \mathbf{C} , i.e., $\mathbf{C} = J^{2/3} \bar{\mathbf{C}}$ (see Section 2.1), the invariants introduced in Equations (71a)–(72b)
719 can be rewritten as $I_1 = J^{2/3} \bar{I}_1$, $I_2 = J^{4/3} \bar{I}_2$, $I_3 = J^2 \bar{I}_3$, $I_4 = J^{2/3} \bar{I}_4$, and $I_5 = J^{4/3} \bar{I}_5$, where
720 the generic \bar{I}_q , with $q = 1, \dots, 5$, is obtained by substituting \mathbf{C} with $\bar{\mathbf{C}}$ in the expression of the
721 corresponding invariant I_q . Clearly, it holds that $\bar{I}_3 = \det \bar{\mathbf{C}} = 1$.

722 Appendix C. Hyperelasticity

723 An elastic material is called hyperelastic if the stress can be obtained by differentiation of a function,
724 called elastic potential or elastic strain energy density, with respect to the conjugated measure of
725 strain/deformation. If the potential is given as a function $W = \hat{W}(\mathbf{C})$ of the right Cauchy-Green
726 deformation \mathbf{C} , the second Piola-Kirchhoff stress is obtained as

$$\mathbf{S} = 2 \frac{\partial \hat{W}}{\partial \mathbf{C}}(\mathbf{C}). \quad (73)$$

727 The Cauchy stress is obtained by means of the forward Piola transformation

$$\boldsymbol{\sigma} = J^{-1} \mathbf{F} \mathbf{S} \mathbf{F}^T = J^{-1} \mathbf{F} \left[2 \frac{\partial \hat{W}}{\partial \mathbf{C}}(\mathbf{C}) \right] \mathbf{F}^T. \quad (74)$$

728 If the material is incompressible, the kinematical constraint $J = 1$ of isochoric (i.e., volume-preserving)
729 motion must be enforced by means of the Lagrange multiplier p (which does *not* have the physical
730 meaning of hydrostatic pressure in this treatment), and the second Piola-Kirchhoff stress tensor is
731 given by

$$\mathbf{S} = -J p \mathbf{B} + 2 \frac{\partial \hat{W}}{\partial \mathbf{C}}(\mathbf{C}), \quad (75)$$

732 where $\mathbf{B} = \mathbf{C}^{-1}$ is the Piola deformation tensor. To obtain the Cauchy stress $\boldsymbol{\sigma}$, a forward Piola
733 transformation is performed on \mathbf{S} , i.e.,

$$\boldsymbol{\sigma} = -p \mathbf{g}^{-1} + J^{-1} \mathbf{F} \left[2 \frac{\partial \hat{W}}{\partial \mathbf{C}}(\mathbf{C}) \right] \mathbf{F}^T, \quad (76)$$

734 where \mathbf{g}^{-1} is the inverse spatial metric tensor, which plays the role of the “contravariant” identity
735 tensor.

736 **Appendix D. Admissible Interval of I_4 or \bar{I}_4**

737 We want to prove that, under a deformation \mathbf{C} , the admissible values of $I_4 = \mathbf{C} : \mathbf{A}$ belong to the
 738 interval $[\lambda_{\min}^2, \lambda_{\max}^2]$, where λ_{\min}^2 and λ_{\max}^2 are the minimum and maximum eigenvalues of \mathbf{C} , for
 739 every $\mathbf{A} = \mathbf{M} \otimes \mathbf{M}$. The same holds for the case of the distortional part $\bar{\mathbf{C}}$ of the deformation, i.e.,
 740 $\bar{I}_4 \in [\bar{\lambda}_{\min}^2, \bar{\lambda}_{\max}^2]$, where $\bar{\lambda}_{\min}^2$ and $\bar{\lambda}_{\max}^2$ are the minimum and maximum eigenvalues of $\bar{\mathbf{C}}$.

741 Let us consider the representation of the deformation \mathbf{C} in terms of its eigenvalues,

$$[\mathbf{C}] = [C_{AB}] = \text{diag}[\lambda_1^2, \lambda_2^2, \lambda_3^2], \quad (77)$$

742 Note that we can write the fourth invariant as

$$I_4 = \mathbf{C} : \mathbf{A} = \mathbf{C} : (\mathbf{M} \otimes \mathbf{M}) = \mathbf{M} \mathbf{C} \mathbf{M} = M^A C_{AB} M^B, \quad (78)$$

743 from which we obtain the equation of an ellipsoid, with matrix $[\frac{1}{I_4} C_{AB}] = \text{diag}[\frac{\lambda_1^2}{I_4}, \frac{\lambda_2^2}{I_4}, \frac{\lambda_3^2}{I_4}]$, i.e.,

$$M^A \left[\frac{1}{I_4} C_{AB} \right] M^B = 1, \quad \Rightarrow \quad \frac{(M^1)^2}{I_4/\lambda_1^2} + \frac{(M^2)^2}{I_4/\lambda_2^2} + \frac{(M^3)^2}{I_4/\lambda_3^2} = 1, \quad (79)$$

744 and semi-axes given by $\sqrt{I_4}/\lambda_\alpha$. If we also impose the fact that \mathbf{M} is a unit vector, we obtain

$$\|\mathbf{M}\|^2 = \mathbf{M} \cdot \mathbf{M} = \mathbf{M} \mathbf{G} \mathbf{M} = M^A G_{AB} M^B = 1. \quad (80)$$

745 Assuming Cartesian coordinates for simplicity of representation, we have that the matrix of the metric
 746 tensor \mathbf{G} reduces to the identity, i.e., $G_{AB} = \delta_{AB}$, and the equation above reduces to the equation of
 747 the unit sphere

$$M^A \delta_{AB} M^B = 1, \quad \Rightarrow \quad (M^1)^2 + (M^2)^2 + (M^3)^2 = 1 \quad (81)$$

748 The admissible values of I_4 are those for which the ellipsoid and the sphere intersect, i.e., the
 749 system of equations given by (79) and (81) admits a solution. Evidently, the minimum value of I_4 is
 750 attained when the *major* semi-axis of the ellipsoid ($\sqrt{I_4}/\lambda_{\min}$) equals the radius of the sphere, i.e.,
 751 $I_4 = \lambda_{\min}^2$ (Figure 7a), and the maximum value of I_4 is attained when the *minor* semi-axis of the
 752 ellipsoid ($\sqrt{I_4}/\lambda_{\max}$) equals the radius of the sphere, i.e., $I_4 = \lambda_{\max}^2$ (Figure 7c). For $I_4 \in \mathring{\Lambda}(\mathbf{C}) =$
 753 $]\lambda_{\min}^2, \lambda_{\max}^2[$, the intersection of the the ellipsoid and the sphere is given by two symmetric curves
 754 (Figure 7b).

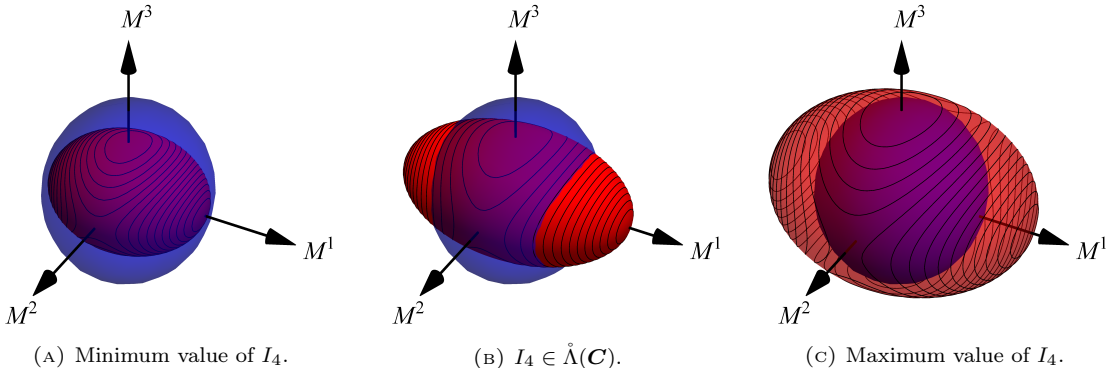


FIGURE 7. Graphical representation of the admissible values of I_4 .

755 Appendix E. Example of Evaluation of the Stress

756 In the INEX and STEx methods, our strategy for the evaluation of the stress was to first expand the
 757 ensemble potential and then differentiate the Taylor-expanded potential with respect to the deformation.
 758 This was aimed at minimising the number of integrals to be performed. As an example, let us
 759 look at the evaluation of the stress for the INEX method, in which, if the incompressibility constraint
 760 $J = 1$ is enforced, we have

$$W_e \simeq \mathcal{G}_n = \hat{\mathcal{G}}_n(\mathbf{C}, \Psi) = \sum_{j=0}^n \frac{1}{j!} \frac{\partial^{(j)} \hat{W}_1}{\partial \bar{I}_4^{(j)}}(1, 1) \sum_{k=0}^j \binom{j}{k} (-1)^k \langle \mathbf{C}^{\otimes(j-k)} | \mathbb{H}_{j-k} \rangle. \quad (82)$$

761 The Cauchy stress is computed according to Equation (76), in which $J = 1$ can be set, i.e.,

$$\boldsymbol{\sigma} = \mathbf{F} \mathbf{S} \mathbf{F}^T = -p \mathbf{g}^{-1} + \mathbf{F} \left[2 \frac{\partial \hat{W}}{\partial \mathbf{C}}(\mathbf{C}) \right] \mathbf{F}^T = -p \mathbf{g}^{-1} + \boldsymbol{\sigma}_c, \quad (83)$$

762 where p is the Lagrange multiplier associated with the condition $J = 1$, and $\boldsymbol{\sigma}_c$ is the constitutive part
 763 of $\boldsymbol{\sigma}$ (here, p is not the hydrostatic pressure, because $\boldsymbol{\sigma}_c$ need not be deviatoric in this formulation of
 764 incompressible hyperelasticity). By using the elastic potential

$$\hat{W}(\mathbf{C}) = \Phi_0 \hat{W}_0(\mathbf{C}) + \Phi_1 \int_{\mathbb{S}^2 \mathcal{B}} \Psi(\mathbf{M}) \hat{W}_1(\mathbf{C}, \mathbf{A}), \quad (84)$$

765 $\boldsymbol{\sigma}_c$ can be written as

$$\begin{aligned} \boldsymbol{\sigma}_c &= \mathbf{F} \left[2\Phi_0 \frac{\partial \hat{W}_0}{\partial \mathbf{C}}(\mathbf{C}) \right] \mathbf{F}^T + \mathbf{F} \left[2\Phi_1 \int_{\mathbb{S}^2 \mathcal{B}} \Psi(\mathbf{M}) \frac{\partial \hat{W}_1}{\partial \mathbf{C}}(\mathbf{C}, \mathbf{A}) \right] \mathbf{F}^T \\ &= \mathbf{F} \left[2\Phi_0 \frac{\partial \hat{W}_0}{\partial \mathbf{C}}(\mathbf{C}) \right] \mathbf{F}^T + \mathbf{F} \left[2\Phi_1 \frac{\partial \hat{W}_e}{\partial \mathbf{C}}(\mathbf{C}) \right] \mathbf{F}^T, \end{aligned} \quad (85)$$

766 where $\hat{W}_e(\mathbf{C}) = \int_{\mathbb{S}^2 \mathcal{B}} \Psi(\mathbf{M}) \hat{W}_1(\mathbf{C}, \mathbf{A})$ is the fibre ensemble elastic potential. Next, $\hat{W}_1(\mathbf{C}, \mathbf{A})$ is written
 767 as the sum of an isotropic and an anisotropic contribution, i.e.,

$$\hat{W}_1(\mathbf{C}, \mathbf{A}) = \hat{W}_{1i}(\mathbf{C}) + \hat{W}_{1a}(\mathbf{C}, \mathbf{A}), \quad (86)$$

768 and the fibre ensemble potential becomes

$$\hat{W}_e(\mathbf{C}) = \hat{W}_{1i}(\mathbf{C}) + \int_{\mathbb{S}^2 \mathcal{B}} \Psi(\mathbf{M}) \hat{W}_{1a}(\mathbf{C}, \mathbf{A}), \quad (87)$$

769 so that $\boldsymbol{\sigma}_c$ takes on the form

$$\boldsymbol{\sigma}_c = \mathbf{F} \left[2\Phi_0 \frac{\partial \hat{W}_0}{\partial \mathbf{C}}(\mathbf{C}) + 2\Phi_1 \frac{\partial \hat{W}_{1i}}{\partial \mathbf{C}}(\mathbf{C}) \right] \mathbf{F}^T + \mathbf{F} \left[2\Phi_1 \int_{\mathbb{S}^2 \mathcal{B}} \Psi(\mathbf{M}) \frac{\partial \hat{W}_{1a}}{\partial \mathbf{C}}(\mathbf{C}, \mathbf{A}) \right] \mathbf{F}^T. \quad (88)$$

770 The general formula (88) should now be specialised according to the approximation method that is
 771 adopted. Since both $\hat{W}_0(\mathbf{C})$ and $\hat{W}_{1i}(\mathbf{C})$ contribute to $\boldsymbol{\sigma}_c$ in the same way for all methods (indeed,
 772 they are independent of the direction of the fibres, and thus need not be approximated by any of our
 773 methods), we can restrict our calculations by focusing on the anisotropic stress contribution of the
 774 fibres only, i.e.,

$$\boldsymbol{\sigma}_{1a} := \mathbf{F} \left[2\Phi_1 \int_{\mathbb{S}^2 \mathcal{B}} \Psi(\mathbf{M}) \frac{\partial \hat{W}_{1a}}{\partial \mathbf{C}}(\mathbf{C}, \mathbf{A}) \right] \mathbf{F}^T. \quad (89)$$

775 Moreover, since the averaging integral in (89) pertains only to the partial second Piola-Kirchhoff stress
 776 tensor

$$\mathbf{S}_{1a} := 2\Phi_1 \int_{\mathbb{S}^2 \mathcal{B}} \Psi(\mathbf{M}) \frac{\partial \hat{W}_{1a}}{\partial \mathbf{C}}(\mathbf{C}, \mathbf{A}), \quad (90)$$

777 it suffices for our purposes to provide, for each of the four proposed approximation methods, the
 778 corresponding approximated expression of \mathbf{S}_{1a} , which we denote by $\mathbf{S}_{1a}^{\text{app}}$. The stress \mathbf{S}_{1a} computed
 779 according to the FESDH method shall be regarded as “exact”.

780 We recall that, for the FESDH method, $\hat{W}_{1a}(\mathbf{C}, \mathbf{A}) = \mathcal{H}(\mathbf{C} : \mathbf{A} - 1)\hat{W}_{1b}(\mathbf{C}, \mathbf{A})$, and \mathbf{S}_{1a} is given
 781 by

$$\mathbf{S}_{1a} = 2\Phi_1 \int_{\mathbb{S}^2\mathcal{B}} \Psi(\mathbf{M}) \mathcal{H}(\mathbf{C} : \mathbf{A} - 1) \frac{\partial \hat{W}_{1b}}{\partial \mathbf{C}}(\mathbf{C}, \mathbf{A}). \quad (91)$$

782 In the FESD, INEX, PARG, and STEx methods, we do not premultiply \hat{W}_{1b} by the Heaviside function,
 783 so that $\hat{W}_{1a}(\mathbf{C}, \mathbf{A}) \equiv \hat{W}_{1b}(\mathbf{C}, \mathbf{A})$ holds true. Thus, with reference to the FESD approximation, $\mathbf{S}_{1a}^{\text{app}}$
 784 is given by

$$\mathbf{S}_{1a}^{\text{app}} = 2\Phi_1 \int_{\mathbb{S}^2\mathcal{B}} \Psi(\mathbf{M}) \frac{\partial \hat{W}_{1a}}{\partial \mathbf{C}}(\mathbf{C}, \mathbf{A}) = 2\Phi_1 \frac{\partial}{\partial \mathbf{C}} \int_{\mathbb{S}^2\mathcal{B}} \Psi(\mathbf{M}) \hat{W}_{1a}(\mathbf{C}, \mathbf{A}). \quad (92)$$

785 For the INEX method, we approximate $\int_{\mathbb{S}^2\mathcal{B}} \Psi(\mathbf{M}) \hat{W}_{1a}(\mathbf{C}, \mathbf{A})$ as

$$\int_{\mathbb{S}^2\mathcal{B}} \Psi(\mathbf{M}) \hat{W}_{1a}(\mathbf{C}, \mathbf{A}) \simeq \sum_{j=0}^n \frac{1}{j!} \frac{\partial^{(j)} \check{W}_{1a}}{\partial \bar{I}_4^{(j)}}(1, 1) \sum_{k=0}^j \binom{j}{k} (-1)^k \langle \mathbf{C}^{\otimes(j-k)} | \mathbb{H}_{j-k} \rangle. \quad (93)$$

786 Consequently, $\mathbf{S}_{1a}^{\text{app}}$ reads

$$\mathbf{S}_{1a}^{\text{app}} = 2\Phi_1 \sum_{j=1}^n \frac{1}{j!} \frac{\partial^{(j)} \check{W}_{1a}}{\partial \bar{I}_4^{(j)}}(1, 1) \sum_{k=0}^{j-1} \binom{j}{k} (-1)^k \frac{\partial}{\partial \mathbf{C}} \langle \mathbf{C}^{\otimes(j-k)} | \mathbb{H}_{j-k} \rangle, \quad (94)$$

787 and one has to compute the derivative

$$\mathbf{T} : \left(\frac{\partial}{\partial \mathbf{C}} \langle \mathbf{C}^{\otimes \ell} | \mathbb{H}_\ell \rangle \right) = \ell \langle \mathbb{H}_\ell | \mathbf{T} \otimes \mathbf{C}^{\otimes(\ell-1)} \rangle, \quad \ell \in \mathbb{N}, \ell \geq 1, n \geq 1, \quad (95)$$

788 where \mathbf{T} is an arbitrary “covariant” second-order tensor. This result can be proven by invoking the
 789 fact that, at least in the case of transverse isotropy, \mathbb{H}_ℓ is fully symmetric for every ℓ , and noticing
 790 that (we show the explicit index calculation only for $\ell = 1, 2$):

$$\frac{\partial}{\partial C_{RS}} \langle \mathbf{C}^{\otimes 1} | \mathbb{H}_1 \rangle = \frac{\partial}{\partial C_{RS}} (C_{MN}(\mathbb{H}_1)^{MN}) = (\mathbb{I}^T)_{MN}{}^{RS} (\mathbb{H}_1)^{MN} = (\mathbb{H}_1)^{RS}, \quad (96)$$

$$\begin{aligned} \frac{\partial}{\partial C_{RS}} \langle \mathbf{C}^{\otimes 2} | \mathbb{H}_2 \rangle &= \frac{\partial}{\partial C_{RS}} (C_{MN} C_{PQ}(\mathbb{H}_2)^{MNPQ}) \\ &= (\mathbb{I}^T)_{MN}{}^{RS} C_{PQ}(\mathbb{H}_2)^{MNPQ} + C_{MN} (\mathbb{I}^T)_{PQ}{}^{RS} (\mathbb{H}_2)^{MNPQ} \\ &= 2(\mathbb{H}_2)^{RSAB} C_{AB}. \end{aligned} \quad (97)$$

791 Therefore, we obtain (again with the help of an arbitrary “covariant” second-order tensor \mathbf{T})

$$\mathbf{T} : \mathbf{S}_{1a}^{\text{app}} = 2\Phi_1 \sum_{j=1}^n \frac{1}{j!} \frac{\partial^{(j)} \check{W}_{1a}}{\partial \bar{I}_4^{(j)}}(1, 1) \sum_{k=0}^{j-1} \binom{j}{k} (-1)^k (j-k) \langle \mathbb{H}_{j-k} | \mathbf{T} \otimes \mathbf{C}^{\otimes(j-k-1)} \rangle. \quad (98)$$

792 For the PARG method, we write $\hat{W}_{1a}(\mathbf{C}, \mathbf{A}) = \mathfrak{f}(\mathcal{P}(\mathbf{C}, \mathbf{A}))$, where \mathfrak{f} is any differentiable function of
 793 its argument, and $\mathcal{P}(\mathbf{C}, \mathbf{A})$ is a tensor-power polynomial. Then, we enforce the approximation

$$\int_{\mathbb{S}^2\mathcal{B}} \Psi(\mathbf{M}) \hat{W}_{1a}(\mathbf{C}, \mathbf{A}) = \int_{\mathbb{S}^2\mathcal{B}} \Psi(\mathbf{M}) \mathfrak{f}(\mathcal{P}(\mathbf{C}, \mathbf{A})) \simeq \mathfrak{f} \left(\int_{\mathbb{S}^2\mathcal{B}} \Psi(\mathbf{M}) \mathcal{P}(\mathbf{C}, \mathbf{A}) \right). \quad (99)$$

794 and $\mathbf{S}_{1a}^{\text{app}}$ becomes

$$\mathbf{S}_{1a}^{\text{app}} = 2\Phi_1 \mathfrak{f}' \left(\int_{\mathbb{S}^2\mathcal{B}} \Psi(\mathbf{M}) \mathcal{P}(\mathbf{C}, \mathbf{A}) \right) \left(\frac{\partial}{\partial \mathbf{C}} \int_{\mathbb{S}^2\mathcal{B}} \Psi(\mathbf{M}) \mathcal{P}(\mathbf{C}, \mathbf{A}) \right). \quad (100)$$

795 In the specific case in which

$$f(\mathcal{P}(\mathbf{C}, \mathbf{A})) = \frac{1}{2}c_{1a} [\exp(\mathcal{P}(\mathbf{C}, \mathbf{A})) - 1] \text{ and } \mathcal{P}(\mathbf{C}, \mathbf{A}) = (\langle \mathbf{C} | \mathbf{A} \rangle - 1)^2,$$

796 so that

$$\int_{\mathbb{S}^2 \mathcal{B}} \Psi(\mathbf{M}) \mathcal{P}(\mathbf{C}, \mathbf{A}) = \langle \mathbf{C}^{\otimes 2} | \mathbb{H}_2 \rangle - 2\langle \mathbf{C} | \mathbb{H}_1 \rangle + 1, \quad (101)$$

797 we obtain

$$\begin{aligned} \mathbf{S}_{1a}^{\text{app}} &= \Phi_1 c_{1a} \exp \left(\int_{\mathbb{S}^2 \mathcal{B}} \Psi(\mathbf{M}) \mathcal{P}(\mathbf{C}, \mathbf{A}) \right) \left(\frac{\partial}{\partial \mathbf{C}} \int_{\mathbb{S}^2 \mathcal{B}} \Psi(\mathbf{M}) \mathcal{P}(\mathbf{C}, \mathbf{A}) \right) \\ &= \Phi_1 c_{1a} \exp \left(\langle \mathbf{C}^{\otimes 2} | \mathbb{H}_2 \rangle - 2\langle \mathbf{C} | \mathbb{H}_1 \rangle + 1 \right) (2\mathbb{H}_2 : \mathbf{C} - 2\mathbb{H}_1). \end{aligned} \quad (102)$$

798 Finally, for the STEx method, if \mathbf{T} is an arbitrary ‘‘covariant’’ second-order tensor, we have

$$\begin{aligned} \mathbf{T} : \mathbf{S}_{1a}^{\text{app}} &= \mathbf{T} : 2\Phi_1 \frac{\partial \hat{W}_{1a}}{\partial \mathbf{C}}(\mathbf{C}, \mathbf{A}) \\ &+ 2\Phi_1 \sum_{j=1}^n \left\langle \frac{1}{j!} \frac{\partial^{(j+1)} \hat{W}_{1a}}{\partial \mathbf{A}^{(j)} \partial \mathbf{C}}(\mathbf{C}, \mathbf{A}_0) \left| \mathbf{T} \otimes \sum_{k=0}^j \left[(-1)^k \binom{j}{k} \text{msym}(\mathbb{H}_{j-k} \otimes \mathbf{A}_0^{\otimes k}) \right] \right. \right\rangle. \end{aligned} \quad (103)$$

799 References

- 800 [1] Y. C. Fung. *Biomechanics. Motion, Flow, Stress, and Growth*. Springer-Verlag, New York, USA, 1990.
- 801 [2] N. M. Bachrach, V. C. Mow, and F. Guilak. Incompressibility of the solid matrix of articular cartilage
802 under high hydrostatic pressures. *Journal of Biomechanics*, 31:445–451, 1998.
- 803 [3] K. El Nady and J. F. Ganghoffer. Computation of the effective mechanical response of biological networks
804 accounting for large configuration changes. *Journal of the Mechanical Behavior of Biological Materials*,
805 58:28–44, 2016.
- 806 [4] D. L. Butler, E. S. Grood, F. R. Noyes, and R. E. Zernicke. Biomechanics of ligaments and tendons.
807 *Exercise and Sport Sciences Reviews*, 6(1):125–182, 1978.
- 808 [5] G. A. Holzapfel, T. C. Gasser, and R. W. Ogden. A new constitutive framework for arterial wall mechanics
809 and a comparative study of material models. *Journal of Elasticity*, 61:1–48, 2000.
- 810 [6] T. C. Gasser, R. W. Ogden, and G. A. Holzapfel. Hyperelastic modelling of arterial layers with distributed
811 collagen fibre orientations. *Journal of the Royal Society Interface*, 3:15–35, 2006.
- 812 [7] C. Bellini and E. S. Di Martino. A mechanical characterization of the porcine atria at the healthy stage
813 and after ventricular tachypacing. *Journal of Biomechanical Engineering*, 134:021008, 2012.
- 814 [8] C. Bellini, E. S. Di Martino, and S. Federico. Mechanical behaviour of the human atria. *Annals of Biomed-*
815 *ical Engineering*, 41:1478–1490, 2013.
- 816 [9] R. M. Aspden and D. W. L. Hukins. Collagen organization in articular cartilage, determined by X-ray
817 diffraction, and its relationship to tissue function. *Proceedings of the Royal Society of London Series B*,
818 212:299–304, 1981.
- 819 [10] J. Mollenhauer, M. Aurich, C. Muehleman, G. Khelashvilli, and T. C. Irving. X-ray diffraction of the
820 molecular substructure of human articular cartilage. *Connective Tissue Research*, 44:201–207, 2003.
- 821 [11] Y. Lanir. Constitutive equations for fibrous connective tissues. *Journal of Biomechanics*, 16:1–12, 1983.
- 822 [12] C. Hurschler, B. Loitz-Ramage, and R. Vanderby Jr. A structurally based stress-stretch relationship for
823 tendon and ligament. *Journal of Biomechanical Engineering*, 119:392–399, 1997.
- 824 [13] K. L. Billiar and M. S. Sacks. Biaxial mechanical properties of the native and glutaraldehyde-treated aortic
825 valve cusp: Part II - A structural constitutive model. *Journal of Biomechanical Engineering*, 122:327–335,
826 2000.
- 827 [14] M. S. Sacks. Incorporation of experimentally-derived fiber orientation into a structural constitutive model
828 for planar collagenous tissues. *Journal of Biomechanical Engineering*, 125:280–287, 2003.
- 829 [15] S. Federico, A. Grillo, and W. Herzog. A transversely isotropic composite with a statistical distribution of
830 spheroidal inclusions: a geometrical approach to overall properties. *Journal of the Mechanics and Physics*
831 *of Solids*, 52:2309–2327, 2004.

- 832 [16] S. Federico and W. Herzog. On the permeability of fibre-reinforced porous materials. *International Journal*
833 *of Solids and Structures*, 45:2160–2172, 2008.
- 834 [17] S. Federico and W. Herzog. Towards an analytical model of soft tissues. *Journal of Biomechanics*, 41:3309–
835 3313, 2008.
- 836 [18] S. Federico and A. Grillo. Elasticity and permeability of porous fibre-reinforced materials under large
837 deformations. *Mechanics of Materials*, 44:58–71, 2012.
- 838 [19] S. Federico. Porous materials with statistically oriented reinforcing fibres. In L. Dorfmann and R. W.
839 Ogden, editors, *Nonlinear Mechanics of Soft Fibrous Materials*, pages 49–120. Springer, Berlin, Germany,
840 2015. CISM Courses and Lectures No. 559, International Centre for Mechanical Sciences.
- 841 [20] S. Federico and T. G. Gasser. Non-linear elasticity of biological tissues with statistical fibre orientation.
842 *Journal of the Royal Society Interface*, 7:955–966, 2010.
- 843 [21] R. H. Hardin and N. J. A. Sloane. McLaren’s improved snub cube and other new spherical designs in
844 three dimensions. *Discrete Computational Geometry*, 15:429–441, 1996.
- 845 [22] V. I. Lebedev. Quadratures on a sphere. *USSR Computational Mathematics and Mathematical Physics*,
846 16:10–24, 1976.
- 847 [23] P. Bažant and B. H. Oh. Efficient numerical integration on the surface of a sphere. *ZAMM, Zeitschrift*
848 *für Angewandte Mathematik und Mechanik (Journal of Applied Mathematics and Mechanics)*, 66:37–49,
849 1986.
- 850 [24] S.-W. Heo and Y. Xu. Constructing fully symmetric cubature formulae for the sphere. *Mathematics of*
851 *Computation*, 70(233):269–279, 2001.
- 852 [25] P. Skacel and J. Bursa. Numerical implementation of constitutive model for arterial layers with distributed
853 collagen fibre orientations. *Computer methods in biomechanics and biomedical engineering*, 18:816–828,
854 2015.
- 855 [26] M. Carfagna and A. Grillo. The spherical design algorithm in the numerical simulation of biological tissues
856 with statistical fibre-reinforcement. Submitted.
- 857 [27] P. J. Flory. Thermodynamic relations for high elastic materials. *Transactions of the Faraday Society*,
858 57:829–838, 1961.
- 859 [28] R. W. Ogden. Nearly isochoric elastic deformations: Application to rubberlike solids. *Journal of the*
860 *Mechanics and Physics of Solids*, 26:37–57, 1978.
- 861 [29] R. W. Ogden. *Non-linear Elastic Deformations*. Dover, New York, USA, 1997.
- 862 [30] K. Kanatani. Stereological determination of structural anisotropy. *International Journal of Engineering*
863 *Science*, 22:531–546, 1984.
- 864 [31] S. G. Advani and C. L. Tucker. The use of tensors to describe and predict fiber orientation in short fiber
865 composites. *Journal of Rheology*, 31:751–784, 1987.
- 866 [32] M. Epstein. *The Geometrical Language of Continuum Mechanics*. Cambridge University Press, Cambridge,
867 UK, 2010.
- 868 [33] R. Segev. Notes on metric independent analysis of classical fields. *Mathematical Methods in the Applied*
869 *Sciences*, 36:497–566, 2013.
- 870 [34] R. H. Hardin, N. J. A. Sloane, and W. D. Smith. *Spherical Codes*. 2008.
871 <http://www.research.att.com/~njas/packings/>.
- 872 [35] Y. Lanir and R. Namani. Reliability of structure tensors in representing soft tissues structure. *Journal of*
873 *the Mechanical Behavior of Biomedical Materials*, 46:222–228, 2015.
- 874 [36] L. J. Walpole. Elastic behavior of composite materials: Theoretical foundations. *Advances in Applied*
875 *Mechanics*, 21:169–242, 1981.
- 876 [37] L. J. Walpole. Fourth-rank tensors of the thirty-two crystal classes: Multiplication tables. *Proceedings of*
877 *the Royal Society of London Series A*, 391:149–179, 1984.
- 878 [38] M. Vasta, A. Gizzi, and A. Pandolfi. On three- and two-dimensional fiber distributed models of biological
879 tissues. *Probabilistic Engineering Mechanics*, 37:170–179, 2014.
- 880 [39] A. Gizzi, A. Pandolfi, and M. Vasta. Statistical characterization of the anisotropic strain energy in soft
881 materials with distributed fibers. *Mechanics of Materials*, 92:119–138, 2016.
- 882 [40] A. M. Römgens, C. C. van Donkelaar, and K. Ito. Contribution of collagen fibers to the compressive
883 stiffness of cartilaginous tissues. *Biomechanics and Modeling in Mechanobiology*, 12:1221–1231, 2013.

- 884 [41] J. M. Mansour. Biomechanics of cartilage. In C. A. Oatis, editor, *Kinesiology: the Mechanics and Path-*
885 *omechanics of Human Movement*, pages 69–83. Lippincott Williams & Wilkins, Philadelphia, USA, second
886 edition, 2009.
- 887 [42] P. Fratzl, K. Misof, I. Zizak, G. Rapp, H. Amenitsch, and S. Bernstorff. Fibrillar structure and mechanical
888 properties of collagen. *Journal of Structural Biology*, 112:119–122, 1997.
- 889 [43] M. Destrade, B. Mac Donald, J. G. Murphy, and G. Saccomandi. At least three invariants are necessary
890 to model the mechanical response of in-compressible, transversely isotropic materials. *Computational*
891 *Mechanics*, 52:959–969, 2013.
- 892 [44] Y. C. Fung. Elasticity of soft tissues in simple elongation. *American Journal of Physiology*, 213:1532–1544,
893 1967.
- 894 [45] J. P. Wilber and J. R. Walton. The convexity properties of a class of constitutive models for biological
895 soft tissues. *Mathematics and Mechanics of Solids*, 7:217–235, 2002.
- 896 [46] J. D. Humphrey. Continuum biomechanics of soft biological tissues. *Proceedings of the Royal Society of*
897 *London Series A*, 459:1–44, 2003.
- 898 [47] S. Federico, A. Grillo, G. Giaquinta, and W. Herzog. Convex Fung-type potentials for biological tissues.
899 *Meccanica*, 43:279–288, 2008.
- 900 [48] A. Tomic, A. Grillo, and S. Federico. Poroelastic materials reinforced by statistically oriented fibres -
901 numerical implementation and application to articular cartilage. *IMA Journal of Applied Mathematics*,
902 79:1027–1059, 2014.
- 903 [49] E. W. Weisstein. Erfi. From MathWorld - A Wolfram Web Resource. 2005.
904 <http://mathworld.wolfram.com/Erfi.html>.
- 905 [50] J. Pajerski. *Nonlinear Biphase Microstructural Numerical Analysis of Articular Cartilage and Chondro-*
906 *cytes*. MSc Thesis, The University of Calgary, Canada, 2010.
- 907 [51] F. dell’Isola and D. J. Steigmann. A two-dimensional gradient-elasticity theory for woven fabrics. *Journal*
908 *of Elasticity*, 118:113–125, 2015.
- 909 [52] D. J. Steigmann and F. dell’Isola. Mechanical response of fabric sheets to three-dimensional bending,
910 twisting, and stretching. *Acta Mechanica Sinica*, 31:373–382, 2015.
- 911 [53] I. Giorgio, R. Grygoruk, F. dell’Isola, and D. J. Steigmann. Pattern formation in the three-dimensional
912 deformations of fibered sheets. *Research Mechanics Communications*, 69:164–171, 2015.
- 913 [54] A. C. Eringen. *Mechanics of Continua*. Robert E. Krieger Publishing Company, Huntington, NY, USA,
914 1980.
- 915 [55] A. J. M. Spencer. Constitutive theory for strongly anisotropic solids. In A. J. M. Spencer, editor, *Contin-*
916 *uum Theory of the Mechanics of Fibre-Reinforced Composites*, pages 1–32. Springer-Verlag, Wien, Austria,
917 1984. CISM Courses and Lectures No. 282, International Centre for Mechanical Sciences.